*Journal of the Geological Society, London*, Vol. **166**, 2009, pp. 999–1012. doi: 10.1144/0016-76492009-038.

# Tectonomagmatic events during stretching and basin formation in the Labrador Sea and the Davis Strait: evidence from age and composition of Mesozoic to Palaeogene dyke swarms in West Greenland

LOTTE M. LARSEN[1]*, LARRY M. HEAMAN[2], ROBERT A. CREASER[2], ROBERT A. DUNCAN[3], ROBERT FREI[4] & MARK HUTCHISON[1]

[1]*Geological Survey of Denmark and Greenland, Øster Voldgade 10, DK-1350 Copenhagen K, Denmark*

[2]*Department of Earth and Atmospheric Sciences, University of Alberta, Edmonton, Alberta, Canada T6G 2E3*

[3]*College of Oceanic and Atmospheric Sciences, Oregon State University, Corvallis, OR 97331, USA*

[4]*Institute of Geology and Geography, University of Copenhagen, Øster Voldgade 10, DK-1350 Copenhagen K, Denmark*

**Corresponding author (e-mail: lml@geus.dk)*

**Abstract:** Mesozoic to Palaeogene intrusive igneous rocks in West Greenland range from a large, coast-parallel dyke swarm to small, poorly defined dyke swarms or single intrusions. New age and geochemical data indicate that intrusion forms and melt compositions changed with time, dependent on changing stress fields and increasing lithospheric attenuation. During the period *c*. 220–150 Ma (Late Triassic to Late Jurassic) incipient stretching is reflected in the production of highly alkaline, volatile-rich melts formed in small volumes in the deep lithosphere. Around 150 Ma (Kimmeridgian), increased extension took place and melts were intruded in a 60 km long swarm of scattered alkaline dykes. In the Early Cretaceous, 140–133 Ma, the regional stress field was intense, upwelling asthenospheric mantle started to melt, and alkali basaltic magmas were emplaced in a 400 km long coastal dyke swarm parallel to large linear faults offshore. In the Palaeocene, continental break-up took place and flood basalts (62–60 Ma) were extruded in the Nuussuaq Basin. Large basalt sills and dykes extend the region with Palaeocene activity 150 km southwards and form a link between the Nuussuaq Basin and the Sisimiut Basin offshore. Dykes with ages of 57–51 Ma indicate widespread younger volcanic activity.

**Supplementary material:** Sample details, Ar/Ar data and plots, and Rb–Sr isochrons are available at http://www.geolsoc.org.uk/SUP18374.

Along the west coast of Greenland several Mesozoic to Palaeogene dyke swarms and other small intrusions occur, with previously reported ages ranging between 28 and *c*. 200 Ma. The magmatism that gave rise to these rocks was presumably causally connected to events of stretching and rifting of the lithosphere before and during the formation of the Labrador Sea and the Davis Strait (e.g. Watt 1969; Hansen 1980). The age, composition, and volume of the magmas were determined by the tectonic environment and the state and composition of the melting mantle, and the dykes therefore preserve a record of plate-tectonic events during the successive stages of rifting and formation of basins offshore West Greenland.

The intrusions vary from a large, coast-parallel dyke swarm to small, poorly exposed dyke swarms and single intrusions that typically have been found during regional geological mapping. Data on these rocks, in particular age data, have been acquired during a long period since 1969 and are of mixed and sometimes uncertain precision. In particular, K–Ar ages may be erroneous if excess argon was present in the dated material.

Recently, high-precision age determinations have been obtained for most of these intrusions, as well as modern geochemical analyses for major and trace elements. As a result, a number of discrete periods of igneous activity and a close connection between ages and chemical compositions have become apparent. This paper presents the results from this work.

## Geological setting

The geotectonic development of the Labrador Sea–Davis Strait region, with stretching, rifting, and subsequent continental break-up between Greenland and Canada, is very complex. Because of the hydrocarbon potential of the basins in the offshore areas, the Labrador Sea and the Davis Strait have been investigated extensively since the early 1970s on both the Greenland and the Canada sides (e.g. overviews by Henderson *et al*. 1981; Balkwill *et al*. 1990; Keen *et al*. 1990; Chalmers & Pulvertaft 2001). Despite the extensive research, which has included geophysical surveys, drilling, and dredging, there has been no unanimous agreement on a model for the history of stretching, rifting, and sea-floor spreading in the region.

The initiation of stretching and basin formation is not well defined. The oldest sediments penetrated by drilling make up the Early Cretaceous Bjarni Formation, of Barremian–Aptian age (130–112 Ma), but the age of an even deeper sequence revealed on seismic sections is not known.

In the spreading models of Srivastava (1978) and Roest & Srivastava (1989), continental break-up and formation of true oceanic crust with linear magnetic anomalies started during geomagnetic chron 33 (83–79 Ma). On the other hand, Chalmers (1991) and Chalmers & Laursen (1995) were unable to model any linear magnetic anomalies older than anomaly 27 and suggested that break-up occurred during geomagnetic chron 27r (62.0–63.1 Ma) (see Fig. 1 and review by Chalmers & Pulvertaft

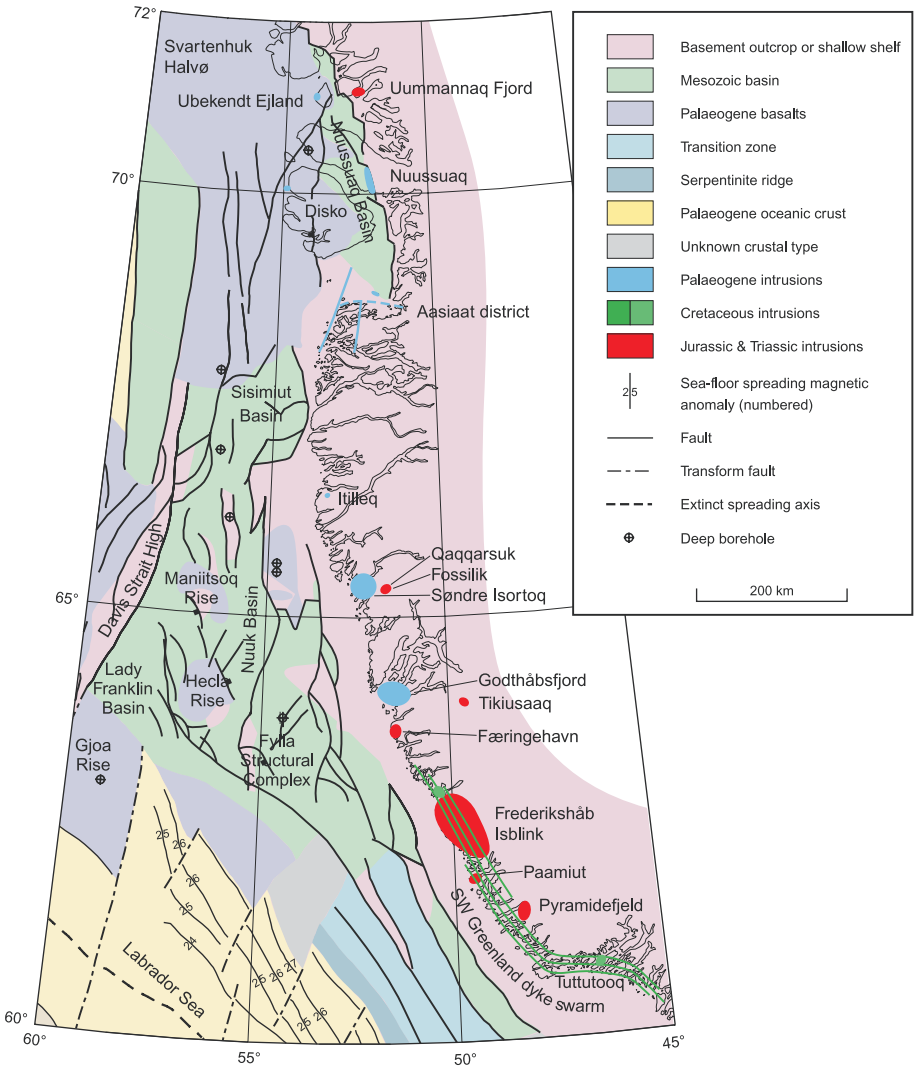


**Fig. 1.** Location of occurrences of Mesozoic–Palaeogene igneous rocks in West Greenland described in this paper. Geology of the offshore areas is modified from Chalmers & Pulvertaft (2001).

2001). More recent work, including drilling of the Qulleq-1 well on the Fylla Bank, has demonstrated the existence of thick Mesozoic sediment accumulations in an area that according to the Roest & Srivastava (1989) model should be oceanic crust (Christiansen *et al*. 2001; Funck *et al*. 2007). There is, in contrast, general agreement on the post-anomaly 27 spreading history.

## Mesozoic to Palaeogene dyke swarms onshore West Greenland

The major part of West Greenland consists of Precambrian basement, thus the age of a dyke swarm or any other undeformed intrusion normally has to be established by radiometric dating. Only intrusions cutting the Cretaceous–Palaeogene sedimentary and volcanic rocks of the Nuussuaq Basin (69°N–73°N) are geologically recognizable as 'young'. The process of identification of young intrusions has been going on continuously since systematic mapping of West Greenland started in the 1940s (e.g. Larsen & Møller 1968; Watt 1969; Bridgwater 1970; Andrews & Emeleus 1971; Hansen & Larsen 1974; Larsen *et al*. 1983, 1999; Larsen & Rex 1992). As late as in 2005 a new carbonatite intrusion was added to the inventory of these rocks (Steenfelt *et al*. 2006; Tappe *et al*. 2009). Several mid- and late Proterozoic intrusions have also been identified (Larsen & Rex 1992; Secher *et al*. 2009). The present paper is, however, solely concerned with Mesozoic to Palaeogene occurrences whose origin may be related to the formation of the Labrador Sea and the Davis Strait. Figure 1 shows the location of the dyke swarms and other intrusions discussed in this paper. A compilation of their emplacement ages is presented in Table 1 and more information has been given by Larsen (2006). Since 2006, a Palaeocene dyke has been found at Itilleq and a Jurassic age has been obtained for a dyke in Uummannaq Fjord. Additional occurrences may be discovered in the future and, in particular, the region north of 72°N is essentially unexplored with regard to young dykes.

The Mesozoic to Palaeogene intrusions show a very large compositional variation. The following rock types are present, listed with decreasing degrees of $SiO_2$ saturation and increasing enrichment in alkalis and volatiles. The rock nomenclature follows Le Maitre (2002) with the modifications to the classification of ultramafic lamprophyres suggested by Tappe *et al*. (2005).

Basaltic rocks and their derivatives (feldspar as phenocrysts and in groundmass): tholeiitic basalt, enriched or transitional basalt, alkali basalt, and phonolite.

Lamprophyres (phenocrysts of one or more of the minerals clinopyroxene, olivine, amphibole, biotite) and carbonatite:

**Table 1.** *Summary, from north to south, of occurrences of Mesozoic–Palaeogene intrusions in West Greenland*

| Locality | Character | Rock type | Method | Age (Ma)[1] | Reference |
|---|---|---|---|---|---|
| Uummannaq Fjord | Few small dykes | Aillikite | Rb–Sr | 186 | 1 |
| Ubekendt Ejland | Small dyke swarm | Camptonite, monchiquite | $^{40}Ar/^{39}Ar$ | 34.5 ± 0.2 | 2 |
| SE Nuussuaq | Dykes and sills, some large | Tholeiitic basalt | $^{40}Ar/^{39}Ar$ | 56.8 ± 0.8 | 1 |
| West of Disko | Volcanic neck | Alkali basalt | $^{40}Ar/^{39}Ar$ | 27.8 ± 0.6 | 2 |
| Western Disko | Regional dyke swarm | Tholeiitic basalt | $^{40}Ar/^{39}Ar$ | 54.3 ± 0.3 | 2 |
| Aasiaat district | Three large dykes, one sill | Tholeiitic basalt | $^{40}Ar/^{39}Ar$ | 56; 61 | 1 |
| Itilleq | One dyke | Tholeiitic basalt | $^{40}Ar/^{39}Ar$ | 64.0 ± 1.3 | 1 |
| Qaqqarsuk | Central complex and dykes | Carbonatite, aillikite | Rb–Sr, U–Pb[2] | *c*. 165 | 3 |
| Fossilik | One explosion breccia | Aillikite | Rb–Sr | 164.2 ± 1.8 | 3 |
| Søndre Isortoq | Small dyke swarm | Camptonite, one alkali basalt | $^{40}Ar/^{39}Ar$ | 56; 58 | 1 |
| Godthåbsfjord | Scattered dykes | Camptonite | $^{40}Ar/^{39}Ar$ | 51.8 ± 0.9 | 1 |
| Tikiusaaq | Central complex and dykes | Carbonatite and aillikite | Rb–Sr, U–Pb[2] | 155–165 | 4 |
| Færingehavn | Few dykes | Aillikite | Rb–Sr, U–Pb | 159; 223[3] | 1 |
| Frederikshåb Isblink | One large dyke | Phonolite | $^{40}Ar/^{39}Ar$ | 106.1 ± 1.5 | 1 |
| Frederikshåb Isblink | Loose dyke swarm | Monchiquite, alnöite, carbonatite | Rb–Sr, U–Pb[2] | 149–152 | 1 |
| Paamiut | Small dyke swarm | Aillikite | K–Ar | 166 ± 5 | 5 |
| Pyramidefjeld[4] | Small dykes and sills | Aillikite | U–Pb | 150–152 | 1, 6 |
| SW Greenland | Large regional dyke swarm | Mildly alkaline basalt | $^{40}Ar/^{39}Ar$ | 133–141 | 1, 7 |
| Tuttutooq | One or a few sills | Camptonite | $^{40}Ar/^{39}Ar$ | 115.4 ± 4.7 | 1 |

References: 1, this work; 2, Storey *et al*. (1998); 3, Secher *et al*. (2009); 4, Tappe *et al*. (2009); 5, Larsen & Møller (1968); 6, Frei *et al*. (2008); 7, Larsen *et al*. (1999). Ages from Storey *et al*. (1998) have been recalculated for an age of the FCT biotite monitor of 28.201 Ma.
[1]Detailed age data for this study are given in Tables 2–4. Errors on single ages are 2$\sigma$.
[2]Samples dated by Rb–Sr or U–Pb dependent on their contents of phlogopite or perovskite.
[3]Rb–Sr ages cited here.
[4]Includes a thick sheet on Midternæs, 16 km NNE of Pyramidefjeld.

camptonite (plagioclase in groundmass and sometimes also as phenocrysts, but also high volatile contents; essentially 'wet' alkali basalts), monchiquite (mafic, no plagioclase; glass or feldspathoid in groundmass), alnöite (ultramafic, carbonate-rich, with melilite), aillikite (ultramafic, carbonate-rich, no melilite), and carbonatite (more than 50% carbonate).

## Dating methods

Samples were dated according to their mineralogy. Basalt, camptonite and phonolite all contain feldspar and were dated by the $^{40}Ar/^{39}Ar$ incremental heating method. Monchiquite, alnöite, aillikite and carbonatite contain phlogopite and sometimes perovskite and were dated by Rb–Sr measurements on separated phlogopite and in some cases bulk rock, and U–Pb measurements on separated perovskite. All decay constants used are those compiled by Steiger & Jäger (1977).

### *$^{40}Ar/^{39}Ar$ analysis*

Ten samples were dated by the $^{40}Ar/^{39}Ar$ incremental heating method in the Noble Gas Mass Spectrometry Laboratory at Oregon State University. The instrument used is a MAP 215-50 rare gas mass spectrometer with all-metal extraction system equipped with a 10 W $CO_2$ laser and Heine low-blank, double-vacuum resistance furnace connected to an ultra-clean, low-volume (*c*. 1000 $cm^3$) gas cleanup line. Samples were degassed in 8–14 temperature steps, from 500 °C to fusion at around 1400 °C. Zr–Al getters removed active gases. Ion beam currents were measured with the electron multiplier at $m/z = 35$, 36, 37, 38, 39, and 40, and intervening baselines. Measurement times, peak/baseline voltages, and data acquisition and storage were computer controlled. Mass discrimination was monitored using zero age basalts. All resulting ages were calculated using the ArArCALC software package (Koppers 2002).

Unaltered phenocrysts were separated by standard mineral separation techniques. Fine-grained, unaltered whole-rocks were cored with a 5 mm diameter diamond-tipped drill bit, then sectioned into discs of 100–300 mg. Samples were irradiated at the Oregon State University TRIGA experimental reactor for 6 h at 1 MW power. The neutron flux was monitored with the FCT-3 biotite monitor. All ages were calculated relative to an age of 28.201 Ma for the Fish Canyon Tuff (Kuiper *et al*. 2008).

### *Rb–Sr analysis*

Three samples from Frederikshåb Isblink were analysed at University of Alberta. Each fraction of separated phlogopite was given a gentle HCl leach to remove entrained carbonate. Isotopic analysis was performed by thermal ionization mass spectrometry (TIMS) using a VG Sector-54 instrument. Full procedural details have been given by Creaser *et al*. (2004). All analyses were corrected relative to an average $^{87}Sr/^{86}Sr$ value of 0.71025 for the SRM 987 Sr standard. For two samples, five phlogopite fractions were analysed per sample and linear regression treatment of the data yielded Model 1 isochron ages (Ludwig 2003). The age of the third sample (one phlogopite fraction) represents a single analysis model age using an assumed initial $^{87}Sr/^{86}Sr$ ratio of 0.7035.

Two samples from Færingehavn and one from Uummannaq Fjord were analysed at the Insitute of Geography and Geology, University of Copenhagen. Sample amounts of 5–10 mg were dissolved for 48 h at 120 °C in concentrated HF together with a mixed, highly enriched $^{87}Rb$–$^{84}Sr$ spike. Isotopic analysis was performed by TIMS on a VG Sector-54 instrument. Sr isotopes were measured in multi-dynamic mode and externally normalized to $^{86}Sr/^{88}Sr = 0.1194$. The external reproducibility of the Sr isotope analyses was controlled by repetitive analyses of the NIST SRM 987 standard, which we measured at $^{87}Sr/^{86}Sr = 0.710238 \pm 17$ ppm. Samples were consequently corrected to the certified value of $^{87}Sr/^{86}Sr = 0.71025$ to allow for inter-laboratory consistency. $^{87}Rb/^{86}Sr$ ratios are precise to better than 2% (2σ). For each sample, bulk rock and one fraction of separated phlogopite were analysed, and the calculated ages are

Model 1 two-point solutions; the resulting initial $^{87}Sr/^{86}Sr$ ratios of 0.7039–0.7052 are similar to those obtained for the samples dated by five-point isochrons, corroborating the correctness of the ages.

### *U–Pb analysis*

Five samples containing perovskite were analysed at University of Alberta. Perovskite was separated by standard crushing and mineral separation techniques as described by Heaman & Kjarsgaard (2000). Perovskite generally occurs as tiny (<80 μm) brown cubes or fragments. Uranium and lead were purified using anion exchange chromatography and their isotopic compositions determined by TIMS using a VG 354 solid source system following the protocol described by Heaman & Kjarsgaard (2000). Lead in the perovskite fractions from Pyramidefjeld and Frederikshåb Isblink contains 26–49% common Pb, and that in perovskite from Færingehavn contains 64–83% common Pb, so a significant common Pb correction has been applied to each analysis. The $^{206}Pb/^{238}U$ ages are least sensitive to the common Pb correction and are reported here. In all cases, the isotopic composition of common Pb present in the perovskite was estimated using the Stacey & Kramers (1975) two-stage crustal evolution model, and a 0.5% uncertainty in the $^{206}Pb/^{204}Pb$ composition was numerically propagated during error calculation.

## Geochemical analyses

Bulk rocks were analysed for major elements by X-ray fluorescence spectrometry (XRF) at GGU/GEUS, following procedures given by Kystol & Larsen (1999), who also presented results for international reference materials. Trace elements were analysed by inductively coupled plasma mass spectrometry (ICP-MS) at GEUS, using a PerkinElmer Elan 6100 DRC Quadrupole mass spectrometer. Sample dissolution followed a modified version of the procedure used by Turner *et al*. (1999) and Ottley *et al*. (2003). Calibration was carried out using two certified REE solutions and three international reference standards supplemented with newer values for the REE. Results for reference samples processed and run simultaneously with the unknowns were normally within 5% of the reference value for most elements with concentrations >0.1 ppm.

## Results

Details of samples and the new age determinations are given in Tables 2–4. Further details are available in the supplementary material. Chemical analyses of representative samples are shown in Table 5; further analyses have been given by Larsen (2006). Variation diagrams illustrating the large compositional variation are shown in Figure 2.

A highly systematic distribution of rock types with age is apparent, as illustrated in Figure 3. The oldest rocks (223–150 Ma) are highly alkaline, volatile-rich and undersaturated ultramafic rocks: aillikite, alnöite and carbonatite. At around 150 Ma the less undersaturated monchiquites were formed, and from 140 Ma onwards the rocks were feldspar-bearing: basalt, camptonite, and phonolite. The Eocene monchiquite is a member of a mainly camptonitic dyke swarm on Ubekendt Ejland (Clarke *et al*. 1983).

## Discussion

### *Melt compositions as indicators of tectonic development*

Melt compositions may be sensitive indicators of the tectonic development of a region. This is because the composition of mantle-derived melt is essentially dependent on three variables: the composition of the melting mantle, and the pressure and temperature at which melting takes place. Beneath an old craton that undergoes stretching and rifting all three factors may vary considerably and give rise to a large range of melt compositions. A systematic tectonic development with time, such as a gradually thinning lithosphere, may thus give rise to a systematic development with time in melt compositions.

The asthenospheric mantle is considered to be of relatively uniform composition regionally because it is convecting (e.g. McDonough & Sun 1995; Salters & Stracke 2004), whereas the subcontinental lithospheric mantle may possess distinct local heterogeneities frozen into it during its long existence. In particular, the subcontinental lithosphere may contain metasomatized regions enriched in volatiles and incompatible elements. These regions contain volatile-bearing minerals such as phlogopite, amphibole and apatite. The volatiles (water and $CO_2$) have a profound influence because they depress the temperature at which melting begins.

The following general petrological scheme is based on

**Table 2.** *$^{40}Ar/^{39}Ar$ ages for feldspar-bearing dykes from West Greenland*

| Locality | Sample number | Material | Plateau age ± 2σ (Ma) | % $^{39}Ar$ | Isochron age ± 2σ (Ma) | MSWD | $^{40}Ar/^{36}Ar$ intercept |
|---|---|---|---|---|---|---|---|
| SE Nuussuaq | 318802 | Whole rock | 56.8 ± 0.8 | 56.2 | 56.8 ± 0.9 | 0.7 | 296 ± 4 |
| Aasiaat district | 455793 | Plagioclase | 60.8 ± 0.8 | 86.5 | 60.6 ± 1.0 | 0.4 | 302 ± 12 |
| Aasiaat district | 464536 | Plagioclase | 56.1 ± 0.2 | 79.0 | 56.3 ± 0.3 | 1.5 | 252 ± 35 |
| Itilleq | 464627 | Plagioclase | 64.0 ± 1.3 | 100 | 64.5 ± 2.0 | 0.3 | 292 ± 12 |
| Søndre Isortoq | KØ17154 | Whole rock | 55.8 ± 0.6 | 39.8 | 55.3 ± 0.8 | 1.9 | 318 ± 25 |
| Søndre Isortoq | KØ17090 | Plagioclase | 58.4 ± 0.6 | 89.1 | 58.1 ± 0.7 | 1.1 | 311 ± 14 |
| Godthåbsfjord | 201449 | Plagioclase | – | 72.3 | 51.8 ± 0.9 | 1.4 | 424 ± 8 |
| Frederikshåb Isblink phonolite | 120403 | Whole rock | 106.1 ± 1.6 | 89.1 | 104.2 ± 3.0 | 1.8 | 309 ± 18 |
| SW Greenland | 26388 | Whole rock | 141.1 ± 2.2 | 79.9 | 141.3 ± 2.3 | 1.4 | 291 ± 28 |
| Tuttutooq | 50068 | Whole rock | – | 77.6 | 115.4 ± 4.7 | 3.4 | 1736 ± 94 |

Sample numbers are GGU numbers except the two samples prefixed KØ; these are from the collections of Kryolitselskabet Øresund. Isochron ages and intercept values are from the inverse isochrons.

**Table 3.** *Rb–Sr age determinations on alkaline dykes from West Greenland*

| Locality | Sample number | Material | Rb (ppm) | Sr (ppm) | $^{87}Rb/^{86}Sr$ | $^{87}Sr/^{86}Sr$ | Age (Ma) | $^{87}Sr/^{86}Sr_i$ |
|---|---|---|---|---|---|---|---|---|
| Uummannaq Fjord | 482915 | Phlogopite | 553 | 108 | 14.908 | 0.74327 (1) | | |
| | 482915 | Whole rock | 129 | 660 | 0.563 | 0.70535 (1) | | |
| | 482915 | *Two-point isochron* | | | | | 185.9 ± 0.1 | 0.70386 (1) |
| Færingehavn | 265872 | Phlogopite | 422 | 485 | 2.502 | 0.71315 (1) | | |
| | 265872 | Whole rock | 124 | 880 | 0.407 | 0.70651 (1) | | |
| | 265872 | *Two-point isochron* | | | | | 222.7 ± 0.3 | 0.70522 (1) |
| Færingehavn | 265877 | Phlogopite | 364 | 279 | 3.779 | 0.71357 (1) | | |
| | 265877 | Whole rock | 86.4 | 1060 | 0.236 | 0.70557 (1) | | |
| | 265877 | *Two-point isochron* | | | | | 158.9 ± 0.2 | 0.70503 (1) |
| Frederikshåb Isblink | 78760A | Phlogopite | 130 | 123 | 3.068 | 0.70992 (2) | | |
| | 78760B | Phlogopite | 296 | 138 | 6.194 | 0.71652 (2) | | |
| | 78760C | Phlogopite | 272 | 155 | 5.097 | 0.71428 (2) | | |
| | 78760D | Phlogopite | 274 | 197 | 4.023 | 0.71207 (2) | | |
| | 78760E | Phlogopite | 271 | 180 | 4.353 | 0.71277 (2) | | |
| | 78760 | *Five-point isochron* | | | | | 149.8 ± 4.4 | 0.7034 (3) |
| Frederikshåb Isblink | 183564A | Phlogopite | 437 | 128 | 9.896 | 0.72454 (4) | | |
| | 183564B | Phlogopite | 373 | 99.7 | 10.85 | 0.72649 (2) | | |
| | 183564C | Phlogopite | 241 | 173 | 4.028 | 0.71207 (2) | | |
| | 183564D | Phlogopite | 229 | 164 | 4.058 | 0.71211 (3) | | |
| | 183564E | Phlogopite | 318 | 152 | 6.051 | 0.71637 (2) | | |
| | 183564 | *Five-point isochron* | | | | | 149.2 ± 2.7 | 0.7035 (2) |
| Frederikshåb Isblink | 183560 | Phlogopite | 245 | 707 | 1.001 | 0.70572 (3) | | |
| | 183560 | *Model age, assuming $^{87}Sr/^{86}Sr$ (i) = 0.7035* | | | | | 156 ± 14 | |

Sample numbers are GGU numbers. Uncertainties quoted are $\pm 2\sigma$ for ages and 2SE for $^{87}Sr/^{86}Sr$ (in parentheses). $^{87}Sr/^{86}Sr_i$ are initial Sr isotope ratios derived from regression.

**Table 4.** *U–Pb age determinations on separated perovskite in alkaline dykes from West Greenland*

| Locality | Sample number | Wt (μg) | U (ppm) | Th (ppm) | Pb (ppm) | Th/U | TCPb (pg) | $^{206}Pb/^{238}U$ | $^{206}Pb/^{238}U$ age (Ma) |
|---|---|---|---|---|---|---|---|---|---|
| Færingehavn | 265872 | 45 | 57 | 235 | 10 | 4.11 | 228 | 0.0344 ± 10 | 217.9 ± 5.8 |
| Færingehavn | 265877 | 48 | 48 | 463 | 25 | 9.63 | 623 | 0.0241 ± 26 | 153.4 ± 16.8 |
| Fr.håb Isblink | 118016 | 69 | 73 | 1064 | 12 | 14.61 | 212 | 0.02388 ± 26 | 152.1 ± 1.6 |
| Pyramidefjeld | 126738 | 151 | 47 | 876 | 4 | 18.62 | 219 | 0.02351 ± 20 | 149.8 ± 1.2 |
| Midternæs* | JA71-20-1 | 53 | 28 | 181 | 3 | 6.56 | 78 | 0.02381 ± 36 | 151.7 ± 2.2 |
| | JA71-20-2 | 80 | 29 | 243 | 4 | 8.47 | 115 | 0.02366 ± 32 | 150.8 ± 2.0 |
| | JA71-20, weighted average of two | | | | | | | | 151.2 ± 1.4 |

*Midternæs is included with the Pyramidefjeld occurrence.
Six-digit sample numbers are GGU numbers. Errors quoted are $2\sigma$. $^{206}Pb/^{238}U$ atomic ratios are corrected for blank, spike and initial common Pb (Stacey & Kramers 1975). Th content is estimated from the amount of $^{208}Pb$ present and the $^{206}Pb/^{238}U$ age. TCPb, total common lead.

numerous experimental studies (e.g. Green & Ringwood 1967; Kushiro 1968), as summarized in textbooks such as those by Wilson (1989) and Best (2006). At high pressures and small degrees of melting the melts will be undersaturated in $SiO_2$ and very rich in volatiles and incompatible elements. With increasing degrees of melting the melts become less undersaturated in $SiO_2$ and less enriched in volatiles and incompatible elements, which become gradually more diluted in the melt. Thus, with increasing degrees of melting the melts change composition from volatile-rich and $SiO_2$-poor to volatile-poor and $SiO_2$-rich, and a generalized melt succession will be (with very approximate degrees of melting in parentheses) carbonatite (<0.5%), ultramafic alkaline silicate melt (aillikite, alnöite) (0.5–1%), strongly undersaturated mafic alkaline melt (monchiquite) (1–4%), alkali basalt including camptonite (4–8%) and tholeiitic basalt (8–20%). This simple succession of melt compositions may at any time be complicated by melting of material with a composition different from that of the asthenospheric mantle. Metasomatized volatile-rich regions in the lithospheric mantle have low melting points and give rise to melts with variable compositions because the source is inhomogeneous, particularly with regard to incompatible trace elements.

Beneath large Archaean cratons such as the North Atlantic craton exposed in West Greenland, the lithosphere is estimated to be around 200–230 km thick (Menzies, 1990; Garrit *et al*. 1997; Sand *et al*. 2009) and does not melt because it is too thick and cold. If the lithosphere becomes stretched and undergoes pressure release or heat addition, or both, low-melting areas may begin to melt. As the lithosphere becomes thinner, the hot asthenosphere will rise beneath the thinned region and start to melt because of the decrease in pressure. With increasing lithospheric thinning and asthenospheric upwelling to shallower levels the degree of melting will increase so that the above-mentioned melt range may be produced. This general relation is seen for West Greenland in a plot of volatiles v. $SiO_2$ (Fig. 4). The volatile-rich, $SiO_2$-poor ultramafic alkaline rocks represent the smallest degrees of melting at the highest pressures, the monchiquites and camptonites are intermediate, and the alkaline to tholeiitic basalts represent the highest degrees of melting at the lowest pressures.

**Table 5.** *Representative analyses of Mesozoic to Palaeogene dykes and small intrusions from West Greenland*

| Area: | Færingehavn | | Uumman. | Qaqqarsuk | Fossilik | Pyramidef | Frederikshåb Isblink | | | SW Greenland dyke swarm | | |
|---|---|---|---|---|---|---|---|---|---|---|---|---|
| Age (Ma): | 223 | 159 | 186 | 165 | 164 | 150 | 152 | 150 | 149 | 141 | 139 | 133 |
| Sample: | 265872 | 265877 | 482915 | 223775 | 409788.1[1] | 126746.12 | 118016[2] | 78760 | 183564[2] | 26388 | 84556 | 45293 |
| Rock type: | Aillikite | Aillikite | Aillikite | Carbonatite | Aillikite | Aillikite | Alnöite | Monchiquite | Monchiquite | Basalt | Basalt | Basalt |
| *Major elements (wt%)* | | | | | | | | | | | | |
| $SiO_2$ | 30.42 | 31.36 | 35.20 | 1.55 | 21.02 | 28.85 | 31.39 | 37.72 | 37.55 | 48.44 | 45.71 | 44.73 |
| $TiO_2$ | 3.97 | 3.74 | 1.06 | 0.02 | 2.68 | 2.91 | 2.79 | 3.58 | 3.92 | 3.32 | 2.75 | 3.98 |
| $Al_2O_3$ | 5.25 | 4.40 | 2.60 | 0.15 | 3.80 | 2.89 | 9.95 | 9.98 | 10.81 | 13.24 | 15.04 | 14.24 |
| $Fe_2O_3$ | 5.35 | 5.36 | 2.75 | 0.20 | 6.38 | 5.50 | 6.48 | 7.65 | 6.12 | 4.28 | 5.14 | 4.40 |
| FeO | 7.24 | 8.17 | 6.04 | 5.17 | 4.79 | 7.14 | 6.50 | 5.98 | 6.31 | 10.24 | 7.32 | 10.11 |
| MnO | 0.21 | 0.21 | 0.16 | 0.62 | 0.25 | 0.19 | 0.39 | 0.20 | 0.15 | 0.23 | 0.21 | 0.23 |
| MgO | 13.56 | 17.96 | 33.96 | 16.35 | 14.10 | 25.64 | 3.67 | 11.05 | 11.43 | 4.68 | 6.29 | 5.00 |
| CaO | 16.79 | 13.06 | 7.15 | 30.05 | 19.44 | 11.05 | 17.55 | 16.32 | 13.47 | 9.29 | 10.81 | 9.09 |
| $Na_2O$ | 1.03 | 0.80 | 0.05 | 0.60 | 0.86 | 0.14 | 5.47 | 1.18 | 1.93 | 3.09 | 2.65 | 3.56 |
| $K_2O$ | 2.47 | 2.32 | 2.07 | 0.14 | 2.44 | 1.27 | 1.57 | 1.02 | 1.99 | 1.37 | 0.87 | 1.36 |
| $P_2O_5$ | 0.35 | 0.71 | 0.44 | 1.02 | 1.43 | 0.40 | 2.43 | 0.50 | 0.51 | 0.45 | 0.70 | 1.42 |
| Volatiles | 12.60 | 11.36 | 7.43 | 43.39 | 21.23 | 13.27 | 11.33 | 3.70 | 5.66 | 1.28 | 2.10 | 1.51 |
| Sum | 99.24 | 99.45 | 98.91 | 99.26 | 98.41 | 99.25 | 99.52 | 98.87 | 99.85 | 99.91 | 99.59 | 99.63 |
| *Trace elements (ppm)* | | | | | | | | | | | | |
| Sc | 54.2 | 23.6 | 11.8 | 9.4 | 19.0 | 18.1 | 14.1 | 35.4 | 35.8 | 29.0 | 27.3 | 23.0 |
| V | 234 | 280 | 103 | 5.7 | 197 | 195 | 212 | 383 | 370 | 348 | 300 | 231 |
| Cr | 249 | 674 | 1598 | | 420 | 1449 | 4.3 | 377 | 265 | 33.1 | 133 | 0.9 |
| Co | 51.0 | 74.8 | 98.1 | 18.8 | 51.1 | 89.8 | 26.8 | 68.1 | 61.4 | 45.0 | 45.4 | 36.6 |
| Ni | 161 | 550 | 1336 | 16.19 | 139 | 858 | 9.48 | 116 | 106 | 41.5 | 76.8 | 9.17 |
| Cu | 143 | 118 | 83.7 | 2.04 | 125 | 76.6 | 28.8 | 106 | 83.5 | 120 | 43.6 | 29.0 |
| Zn | 91.8 | 102 | 48.4 | 19.5 | 107 | 93.1 | 194 | 102 | 92.1 | 144 | 96.8 | 131 |
| Ga | 17.1 | 14.5 | 5.33 | 3.08 | 15.4 | 11.9 | 26.5 | 16.4 | 17.7 | 22.8 | 19.4 | 20.3 |
| Rb | 116 | 88.1 | 114 | 3.26 | 82.4 | 48.3 | 85.2 | 29.1 | 63.1 | 34.1 | 14.1 | 28.5 |
| Sr | 868 | 1034 | 655 | 5693 | 2873 | 836 | 2892 | 862 | 607 | 400 | 581 | 875 |
| Y | 42.9 | 22.6 | 4.46 | 21.3 | 31.6 | 12.5 | 61.7 | 19.1 | 17.4 | 41.3 | 23.4 | 31.1 |
| Zr | 544 | 355 | 64.5 | 4.8 | 874 | 181 | 710 | 194 | 185 | 294 | 98.7 | 165 |
| Nb | 173 | 137 | 132 | 434 | 283 | 108 | 359 | 98.2 | 79.6 | 64.4 | 23.7 | 45.8 |
| Cs | 2.89 | 1.20 | 5.94 | 0.040 | 1.16 | 1.47 | 0.733 | 0.446 | 0.671 | 1.88 | 0.158 | 1.031 |
| Ba | 1236 | 820 | 979 | 208 | 1328 | 502 | 1599 | 503 | 778 | 418 | 817 | 755 |
| La | 161 | 91.15 | 119 | 146 | 256 | 75.6 | 256 | 62.2 | 50.8 | 44.4 | 22.2 | 44.9 |
| Ce | 323 | 188.50 | 203 | 319 | 498 | 151 | 511 | 128 | 105 | 93.5 | 48.2 | 95.0 |
| Pr | 39.8 | 24.3 | 21.1 | 35.7 | 56.5 | 18.6 | 61.5 | 15.6 | 13.2 | 12.4 | 6.5 | 12.9 |
| Nd | 138 | 90.2 | 64.9 | 133 | 197 | 69.1 | 216 | 57.6 | 49.7 | 48.6 | 28.1 | 52.8 |
| Sm | 19.5 | 15.1 | 6.39 | 18.2 | 26.4 | 10.5 | 32.8 | 9.67 | 8.47 | 9.85 | 6.17 | 9.98 |
| Eu | 4.67 | 3.84 | 1.41 | 4.69 | 6.9 | 2.84 | 8.58 | 2.64 | 2.38 | 2.90 | 2.92 | 3.59 |
| Gd | 14.6 | 11.3 | 4.05 | 13.0 | 20.6 | 6.60 | 27.2 | 7.70 | 6.97 | 8.69 | 5.39 | 8.48 |
| Tb | 1.66 | 1.31 | 0.399 | 1.54 | 2.43 | 0.87 | 3.14 | 0.897 | 0.844 | 1.38 | 0.839 | 1.19 |
| Dy | 8.27 | 6.04 | 1.50 | 7.52 | 10.1 | 3.78 | 14.9 | 4.45 | 4.22 | 7.83 | 4.54 | 6.28 |
| Ho | 1.50 | 0.912 | 0.184 | 1.06 | 1.26 | 0.544 | 2.32 | 0.728 | 0.657 | 1.60 | 0.860 | 1.20 |
| Er | 4.45 | 2.07 | 0.466 | 2.69 | 3.52 | 1.03 | 5.88 | 1.74 | 1.61 | 3.99 | 2.15 | 2.84 |
| Tm | 0.69 | 0.237 | 0.046 | 0.26 | 0.330 | 0.106 | 0.733 | 0.208 | 0.200 | 0.608 | 0.299 | 0.387 |
| Yb | 4.27 | 1.202 | 0.243 | 1.4 | 1.91 | 0.626 | 4.28 | 1.22 | 1.10 | 3.43 | 1.75 | 2.25 |
| Lu | 0.636 | 0.153 | 0.040 | 0.169 | 0.240 | 0.075 | 0.624 | 0.174 | 0.159 | 0.494 | 0.252 | 0.322 |
| Hf | 16.9 | 9.25 | 1.43 | 0.28 | 14.6 | 5.04 | 14.2 | 4.90 | 5.06 | 7.33 | 2.55 | 4.08 |
| Ta | 10.1 | 8.25 | 7.75 | 221 | 14.0 | 8.16 | 23.3 | 6.27 | 5.17 | 3.97 | 1.44 | 2.82 |
| Pb | 5.05 | 6.41 | 9.29 | 8.86 | 8.14 | 3.38 | 15.7 | 3.78 | 2.96 | 3.80 | 1.49 | 3.84 |
| Th | 56.2 | 12.0 | 20.9 | 1.43 | 15.4 | 8.21 | 32.7 | 6.94 | 5.70 | 5.21 | 1.74 | 3.72 |
| U | 11.0 | 2.50 | 3.01 | 249 | 5.06 | 2.02 | 10.1 | 1.90 | 1.31 | 1.40 | 0.477 | 1.06 |

| Area: | Tuttutooq | Fr. Isblink | Itilleq | Søndre Isortoq | | | Godthåbsfjord | | Aasiaat region | | Nuussuaq | Ub. Ejland |
|---|---|---|---|---|---|---|---|---|---|---|---|---|
| Age (Ma): | 115 | 106 | 64 | 58.5 | 55.7 | | 51.7 | | 60.9 | 56.1 | 56.8 | 34.5 |
| Sample: | 50071 | 120403 | 464627[2] | KØ 17088[3] | KØ 17154 | KØ 15927 | 201449 | 265896 | 455791 | 464536[4] | 318712[5] | 265895[6] |
| Rock type: | Camptonite | Phonolite | Tho.basalt | Alk basalt | Camptonite | Camptonite | Camptonite | Camptonite | Tho.basalt | Tho.basalt | Tho.basalt | Monchiquite |
| *Major elements (wt%)* | | | | | | | | | | | | |
| $SiO_2$ | 43.42 | 60.52 | 46.08 | 44.69 | 45.11 | 42.52 | 47.09 | 46.54 | 48.17 | 48.43 | 47.94 | 41.20 |
| $TiO_2$ | 2.96 | 0.80 | 1.34 | 2.52 | 1.76 | 1.05 | 1.17 | 1.24 | 2.11 | 4.08 | 3.70 | 1.23 |
| $Al_2O_3$ | 16.48 | 17.04 | 17.23 | 15.60 | 16.30 | 12.16 | 15.94 | 16.57 | 14.63 | 12.55 | 13.11 | 14.53 |
| $Fe_2O_3$ | 5.49 | 3.64 | 4.30 | 6.20 | 2.95 | 3.20 | 3.13 | 3.47 | 5.29 | 5.52 | 4.18 | 2.84 |
| FeO | 7.10 | 0.40 | 7.49 | 6.23 | 6.58 | 5.86 | 6.37 | 5.96 | 7.51 | 9.98 | 10.77 | 5.64 |
| MnO | 0.23 | 0.43 | 0.17 | 0.20 | 0.21 | 0.22 | 0.14 | 0.15 | 0.19 | 0.24 | 0.23 | 0.18 |
| MgO | 5.18 | 0.39 | 8.30 | 5.91 | 5.87 | 11.38 | 4.22 | 6.66 | 5.91 | 4.40 | 5.36 | 8.12 |
| CaO | 7.40 | 0.54 | 8.77 | 8.35 | 11.50 | 13.37 | 8.67 | 10.03 | 11.54 | 9.09 | 9.45 | 12.17 |
| $Na_2O$ | 4.21 | 8.09 | 2.81 | 3.27 | 2.93 | 1.48 | 3.63 | 2.61 | 2.59 | 2.75 | 2.46 | 3.49 |
| $K_2O$ | 2.39 | 5.67 | 0.12 | 0.77 | 1.48 | 1.00 | 2.18 | 1.15 | 0.28 | 1.20 | 1.21 | 2.53 |
| $P_2O_5$ | 0.55 | 0.13 | 0.15 | 0.96 | 0.45 | 0.32 | 0.45 | 0.18 | 0.19 | 0.53 | 0.54 | 0.45 |
| Volatiles | 4.65 | 1.68 | 2.39 | 4.60 | 4.64 | 6.80 | 6.13 | 4.71 | 1.63 | 1.33 | 0.60 | 6.78 |
| Sum | 100.05 | 99.33 | 99.15 | 99.29 | 99.78 | 99.36 | 99.11 | 99.28 | 100.03 | 100.11 | 99.56 | 99.16 |
| *Trace elements (ppm)* | | | | | | | | | | | | |
| Sc | 18.4 | 4.7 | 29.4 | 31.0 | 35.3 | 25.7 | 23.6 | 27.2 | 40.7 | 31.2 | 30.7 | 26.3 |
| V | 247 | 20 | 198 | 261 | 229 | 171 | 134 | 198 | 438 | 411 | 387 | 218 |
| Cr | 6.9 | 0.0 | 75.9 | 107 | 257 | 819 | 130 | 191 | 98.2 | 16.5 | 48.7 | 315 |
| Co | 42.8 | 11.0 | 69.0 | 50.5 | 41.7 | 58.6 | 40.2 | 50.0 | 45.2 | 93.5 | 45.2 | 40.3 |
| Ni | 5.68 | 0.29 | 167 | 89.6 | 65.3 | 458 | 87.4 | 137 | 77.8 | 31.3 | 46.9 | 131 |
| Cu | 22.2 | 2.34 | 104 | 68.9 | 82.1 | 72.0 | 52.5 | 76.1 | 250 | 190 | 207 | 94.1 |
| Zn | 152 | 180 | 85.7 | 103 | 59.1 | 53.2 | 66.3 | 63.5 | 107 | 147 | 148 | 66.5 |
| Ga | 22.3 | 38.2 | 16.0 | 20.2 | 16.5 | 11.8 | 15.7 | 14.4 | 21.3 | 23.0 | 23.5 | 14.4 |
| Rb | 63.8 | 183.4 | 2.02 | 14.4 | 38.3 | 35.0 | 76.5 | 43.5 | 3.39 | 25.8 | 32.1 | 78.4 |
| Sr | 908 | 8.82 | 293 | 560 | 752 | 738 | 881 | 645 | 242 | 334 | 392 | 811 |
| Y | 29.4 | 76.9 | 31.0 | 49.6 | 28.0 | 17.8 | 26.3 | 23.5 | 33.2 | 45.9 | 47.5 | 21.4 |
| Zr | 270 | 1010 | 84.0 | 268 | 161 | 99.7 | 145 | 96.7 | 111 | 283 | 269 | 109 |
| Nb | 80.4 | 356 | 2.38 | 47.7 | 72.3 | 46.0 | 66.5 | 30.0 | 6.30 | 44.9 | 59.2 | 138 |
| Cs | 13.65 | 1.016 | 0.066 | 0.316 | 0.398 | 0.757 | 0.733 | 1.110 | 0.046 | 0.115 | 0.535 | 0.994 |
| Ba | 871 | 5.64 | 127 | 882 | 954 | 877 | 1026 | 287 | 40.9 | 317 | 488 | 1697 |
| La | 58.1 | 277 | 6.74 | 86.8 | 62.5 | 33.0 | 84.7 | 22.2 | 6.33 | 31.7 | 41.5 | 84.6 |
| Ce | 115 | 490 | 16.6 | 161 | 114 | 60.7 | 151 | 43.2 | 17.6 | 68.0 | 87.4 | 139 |
| Pr | 14.9 | 52.8 | 2.48 | 18.6 | 13.0 | 7.27 | 15.4 | 5.51 | 2.79 | 10.0 | 11.3 | 14.9 |
| Nd | 55.0 | 153 | 12.1 | 66.5 | 44.6 | 26.6 | 48.5 | 20.3 | 14.0 | 41.1 | 47.7 | 50.6 |
| Sm | 10.0 | 20.1 | 3.60 | 10.9 | 6.73 | 4.11 | 6.50 | 3.91 | 4.40 | 9.42 | 10.1 | 6.99 |
| Eu | 2.85 | 2.42 | 1.35 | 3.16 | 2.04 | 1.35 | 1.82 | 1.26 | 1.58 | 2.83 | 3.11 | 2.02 |
| Gd | 8.06 | 18.4 | 4.16 | 10.1 | 6.34 | 3.80 | 6.13 | 3.98 | 5.29 | 10.6 | 11.0 | 5.65 |
| Tb | 1.12 | 2.32 | 0.766 | 1.52 | 0.922 | 0.571 | 0.878 | 0.637 | 0.922 | 1.54 | 1.61 | 0.743 |
| Dy | 5.77 | 13.3 | 4.70 | 8.68 | 5.19 | 3.19 | 4.77 | 3.95 | 5.66 | 8.38 | 8.45 | 4.08 |
| Ho | 1.12 | 2.64 | 1.06 | 1.80 | 1.06 | 0.657 | 0.919 | 0.849 | 1.215 | 1.74 | 1.63 | 0.824 |
| Er | 2.81 | 7.48 | 2.85 | 4.71 | 2.74 | 1.74 | 2.48 | 2.25 | 3.24 | 4.25 | 4.22 | 2.06 |
| Tm | 0.383 | 1.16 | 0.433 | 0.711 | 0.418 | 0.259 | 0.364 | 0.340 | 0.456 | 0.674 | 0.582 | 0.299 |
| Yb | 2.29 | 7.10 | 2.66 | 4.16 | 2.53 | 1.61 | 2.33 | 2.07 | 2.92 | 3.77 | 3.52 | 1.91 |
| Lu | 0.333 | 1.11 | 0.411 | 0.642 | 0.379 | 0.235 | 0.366 | 0.329 | 0.443 | 0.571 | 0.532 | 0.282 |
| Hf | 6.46 | 22.5 | 2.39 | 5.84 | 3.71 | 2.33 | 3.42 | 2.37 | 3.00 | 6.90 | 6.24 | 2.59 |
| Ta | 5.62 | 21.4 | 0.829 | 2.49 | 4.54 | 2.92 | 2.86 | 1.53 | 0.452 | 3.38 | 3.14 | 6.63 |
| Pb | 24.5 | 22.8 | 1.45 | 5.61 | 3.84 | 2.67 | 6.20 | 1.56 | 3.46 | 2.07 | 1.44 | 6.12 |
| Th | 5.94 | 31.4 | 0.218 | 6.67 | 6.80 | 3.26 | 9.01 | 1.90 | 0.468 | 3.20 | 4.27 | 10.8 |
| U | 3.03 | 6.81 | 0.049 | 1.63 | 1.50 | 0.737 | 1.97 | 0.390 | 0.158 | 0.994 | 1.25 | 2.33 |

Major elements mainly by XRF; $Na_2O$ by atomic absorption spectrometry and FeO by titration. 'Volatiles' is loss on ignition corrected for oxygen uptake. Trace elements determined by ICP-MS.
[1]From Hansen (2002). [2]Major elements from Hansen (1979). [3]Same dyke as the dated sample KØ17090. [4]From Árting (2004). [5]Same intrusion as the dated sample 318802. [6]Chilled margin of sample UE500 dated by Storey *et al.* (1998).

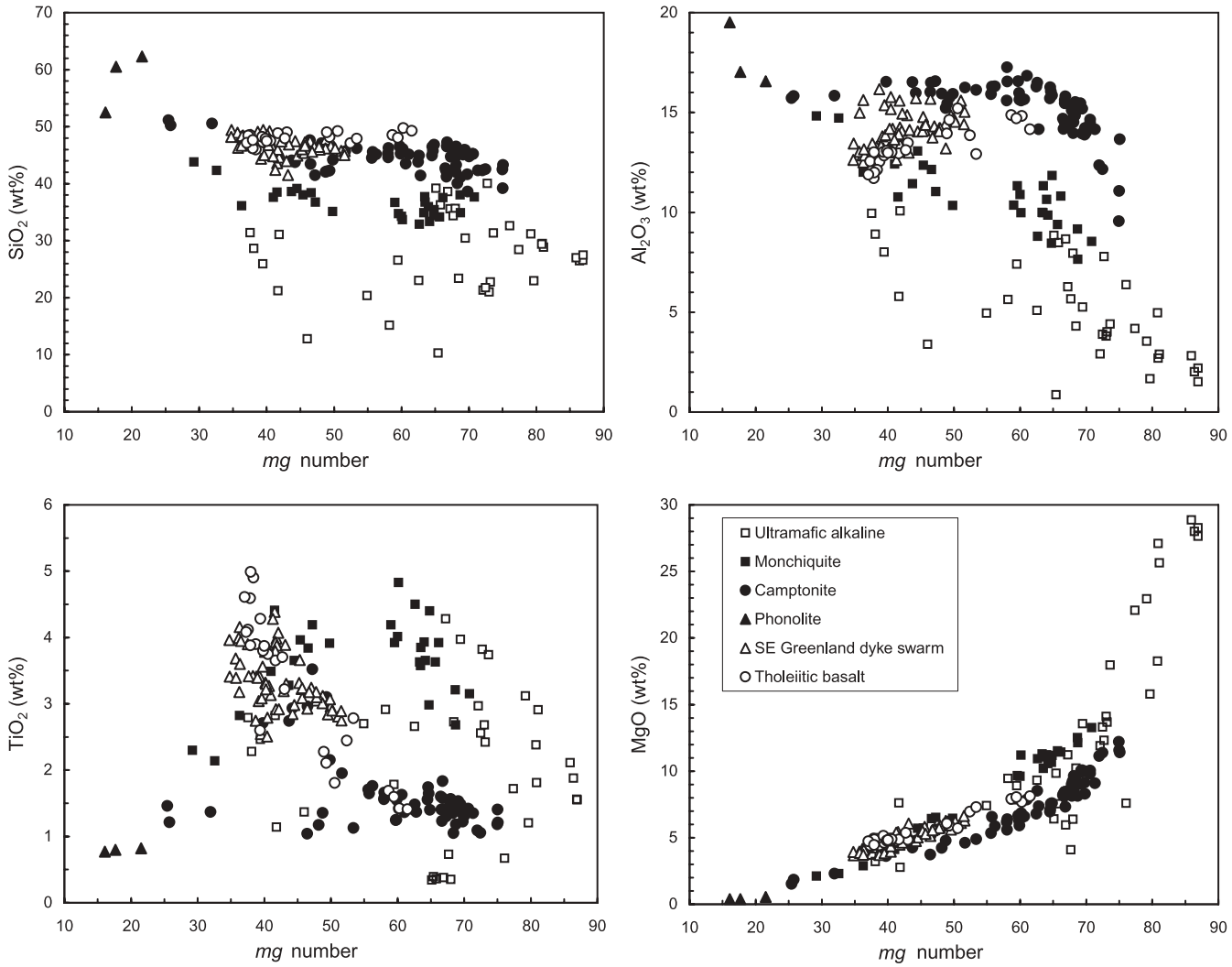


**Fig. 2.** Major element variation diagrams for the Mesozoic–Palaeogene igneous rocks in West Greenland, illustrating the large compositional variation present. The ultramafic alkaline group comprises aillikites, alnöites and carbonatites. The *mg*-number is atomic 100 × Mg/(Mg + $Fe^{2+}$), with the iron oxidation ratio adjusted to $Fe_2O_3/FeO = 0.15$. Because the magmas have high primary contents of volatile elements (mainly $H_2O$ and $CO_2$), the plotted analyses are not recalculated volatile-free.

### *Melts from asthenospheric mantle and metasomatized mantle*

A characteristic feature of the strongly enriched (in incompatible elements and volatiles) and alkaline carbonatites, aillikites, alnöites and monchiquites is that they show a large compositional scatter in many chemical diagrams such as those in Figures 2 and 5. This can be ascribed partly to mineral accumulation effects that make the bulk-rock compositions deviate from the original melt compositions, and partly to melt variations produced in a heterogeneous mantle source. Figure 5 shows La/Sm plotted against $K_2O/SiO_2$. Both these ratios have the more incompatible element in the nominator and are therefore high at low degrees of melting, and both ratios are sensitive to mantle metasomatism. In this plot, tholeiitic and mildly alkaline basalts form a positively correlated, tight array, which must be due to mantle melting systematics as the ratios are not sensitive to later fractional crystallization. This suggests that all the basaltic rocks (the Cretaceous dyke swarm in SW Greenland and the Palaeogene syn- to post-volcanic basalt dykes in the Aasiaat–Disko–Nuussuaq region) arose in very similar mantle, which would most probably be the asthenosphere. The tholeiitic basalts were formed at the largest degrees of melting and the mildly alkaline SW Greenland dyke swarm at the smallest. On the other hand, the camptonites, monchiquites, aillikites, alnöites and carbonatites show a large data scatter and have strongly increased La/Sm and $K_2O/SiO_2$ ratios indicating that they originated in a La- and K-metasomatized mantle.

In conclusion, the tholeiitic and mildly alkaline basalts are interpreted as derived from unmodified asthenospheric mantle, whereas the more alkaline rocks include a metasomatic component from either the lithosphere or the asthenosphere.

### *Degrees of melting*

The behaviour of the REE during mantle melting can be modelled as a function of the melting mineral assemblage (lherzolite: olivine + orthopyroxene + clinopyroxene, with garnet (deeper than *c*. 80 km) or with spinel (shallower than *c*. 80 km)), the composition of the mantle, and the degree of melting. Figure 6 shows the results of such modelling, with the mantle composi-

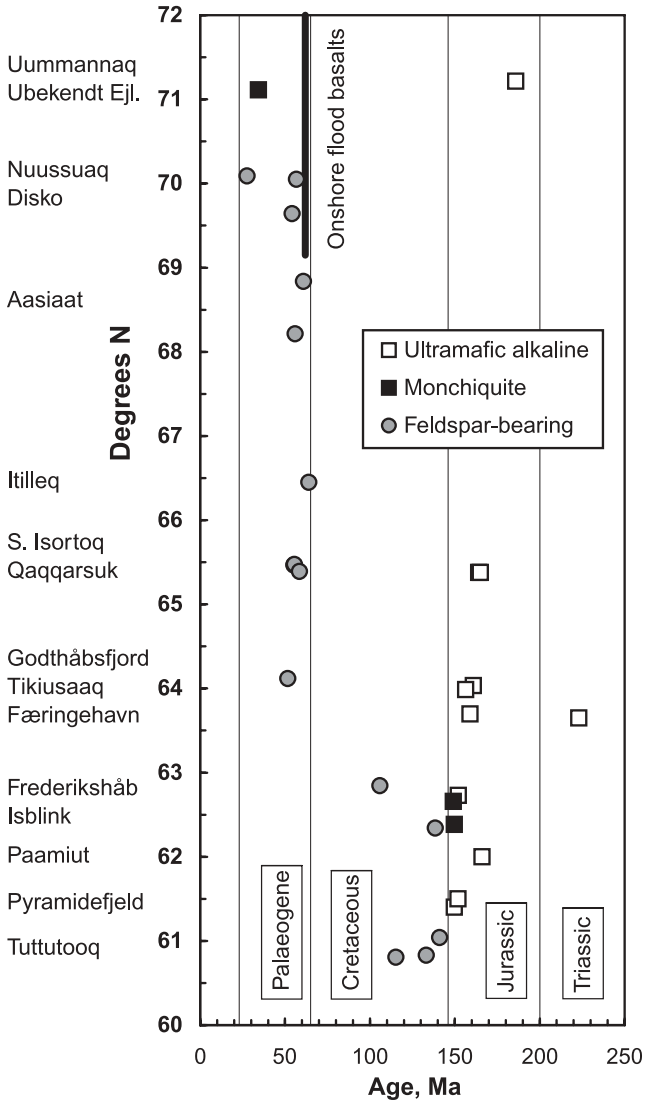


**Fig. 3.** Geographical latitude v. precise age determinations for the Mesozoic–Palaeogene igneous rocks in West Greenland. The ultramafic alkaline group comprises aillikites, alnöites and carbonatites. The mafic alkaline group comprises only the feldspar-free monchiquites. The feldspar-bearing group comprises tholeiitic basalts, alkali basalts, camptonites and phonolite. Age data include results from Storey *et al*. (1998), Larsen *et al*. (1999), Secher *et al*. (2009) and Tappe *et al*. (2009). (See also Table 1.)

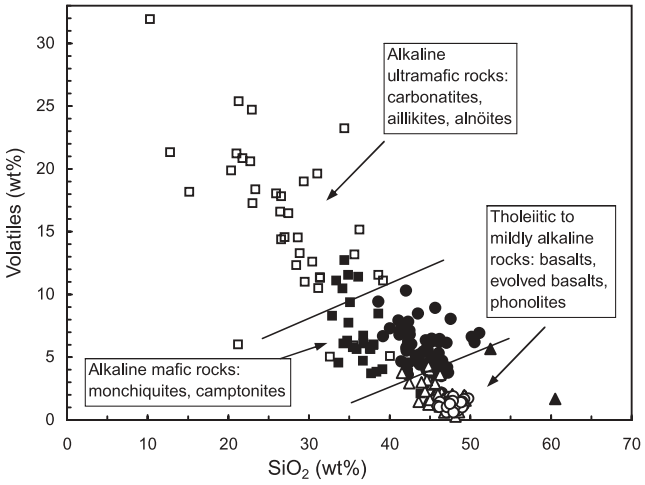


**Fig. 4.** Volatiles v. $SiO_2$ for the Mesozoic–Palaeogene igneous rocks in West Greenland. The lines divide the diagram into fields of alkaline ultramafic rocks (aillikites, alnöites and carbonatites), alkaline mafic rocks (monchiquites and camptonites), and basalts (both mildly alkaline and tholeiitic), with some overlap between fields. Symbols as in Figure 2.

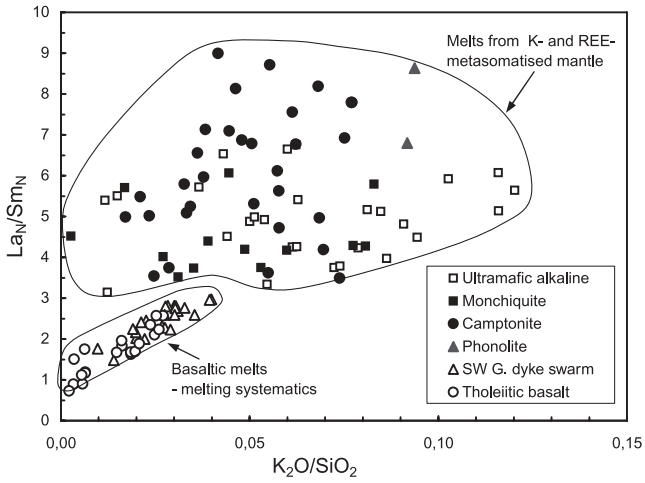


**Fig. 5.** Ratios of light to intermediate REE (La/Sm) v. $K_2O/SiO_2$. The La/Sm ratio is normalized against chondrite concentrations (from McDonough & Sun 1995).

tion chosen as similar to chondritic meteorites. If a more depleted mantle is chosen, such as is believed to constitute the asthenospheric mantle, the curve for garnet-facies melting will move to lower Dy/Yb ratios. It is seen that no melts have Dy/Yb ratios corresponding to an origin solely within spinel-facies mantle. At the other end, all the ultramafic alkaline rocks and monchiquites have Dy/Yb ratios that are impossibly high even for the chondritic mantle model, and melting of an enriched metasomatized mantle is indicated in accordance with the conclusions reached from Figure 5. The degrees of melting would have been less than about 2%. The tholeiitic and mildly alkaline basalts from the SW Greenland dyke swarm form a trend that suggests derivation from more uniform mantle material; the melting could either be solely in garnet facies (for a more depleted mantle than shown here) or in a mixed garnet–spinel facies, where the melting started in garnet facies and continued through the garnet–spinel transition. The degrees of melting indicated are lowest for the mildly alkaline Cretaceous dyke swarm (3–5% in this model) and highest for the tholeiitic Palaeocene Aasiaat–Disko–Nuussuaq dykes (5 to >10%). The camptonites all have low Dy/Yb ratios corresponding to significant melting in spinel facies; however, it is also possible that the camptonites originated in a metasomatized mantle with amphibole as a residual phase or that they have fractionated amphibole; this would invalidate the REE modelling.

## *Depths of melting*

Depths of melting of the investigated rocks can only be crudely estimated. In general, melting at higher pressures leads to more iron-rich melts (Kushiro 1968), and thus the iron content of a mantle-derived melt may be used as a pressure indicator. The iron content is not very sensitive to the degree of melting, but

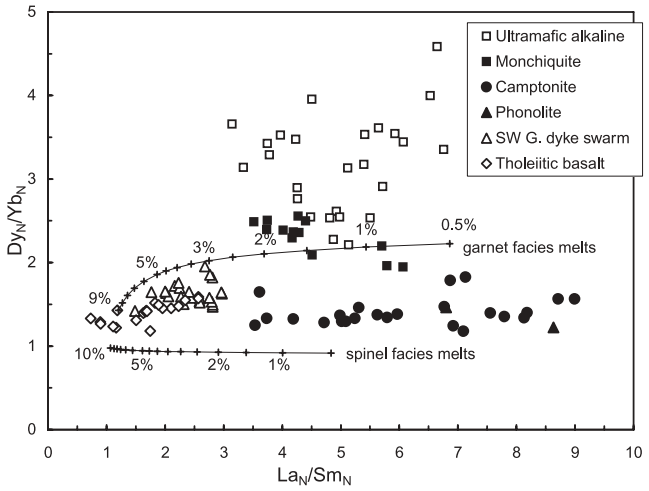


**Fig. 6.** Rare earth element ratio plot (chondrite-normalized) with modelling of mantle lherzolite melting in garnet and spinel facies. The melting model is similar to that of Duggen *et al*. (2005) for a chondritic undepleted mantle. Use of a depleted mantle will shift the garnet-facies curve to lower Dy/Yb ratios. The numbers are per cent melt formed.

fractional crystallization leads to an increase and subsequent decrease in iron. In the FeO v. $SiO_2$ diagram shown in Figure 7, the effects of melting pressure and subsequent fractionation are superimposed because many samples represent fairly fractionated melts (e.g. the highly fractionated phonolites with very low iron contents and high $SiO_2$). However, one feature is robust: the camptonites all have significantly lower iron contents than the 'dry' basaltic rocks, even though they represent broadly similar degrees of fractionation. In accordance with the REE modelling results (Fig. 6), this suggests that the camptonites were generated at significantly lower pressures than the basalts. Compared with experimentally produced volatile-free melts (Walter 1998), the high-iron melts could have been produced at around 50 kbar pressure (*c*. 160 km depth) and the low-iron melts at around 30 kbar pressure (*c*. 100 km depth). The basalts are fairly fractionated rocks, and if they have been enriched in iron as a result of

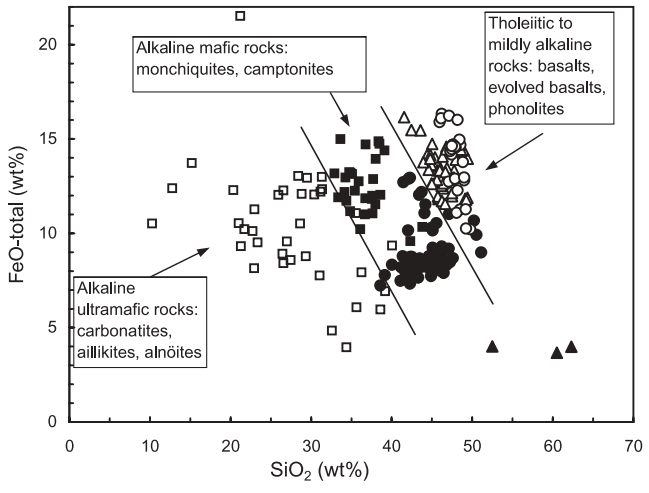


**Fig. 7.** Total iron v. $SiO_2$ for the Mesozoic–Palaeogene igneous rocks in West Greenland. The lines divide the diagram into fields of alkaline ultramafic rocks (aillikites, alnöites and carbonatites), alkaline mafic rocks (monchiquites and camptonites), and basalts (both mildly alkaline and tholeiitic), with some overlap between fields. Symbols as in Figure 6.

fractionation, as is likely, then the pressures of generation for these are overestimated. The high iron contents in most of the primitive alkaline ultramafic rocks and monchiquites indicate high pressures of generation, but it is difficult to compare quantitatively with the much more siliceous volatile-free experimental melts.

In conclusion, the pressure estimates suggest that the rocks generated at the highest pressures are the Triassic–Jurassic aillikites, alnöites and carbonatites of Pyramidefjeld, Paamiut, Frederikshåb Isblink, Færingehavn, Tikiusaaq, Fossilik, Qaqqarsuk and Uummannaq Fjord. The iron-rich monchiquites of Frederikshåb Isblink and the Cretaceous SW Greenland basalt dyke swarm were probably also generated at relatively high pressures. The rocks generated at the lowest pressures are the camptonites of Godthåbsfjord and Søndre Isortoq and the camptonites and monchiquites of Ubekendt Ejland.

### *Relation between magmatism and tectonic development of the Labrador Sea and Davis Strait*

In Figure 3, a systematic evolution of the melt types with time is apparent. There is also a significant spatial distribution of ages: all the Triassic–Cretaceous occurrences except Qaqqarsuk–Fossilik and Uummannaq Fjord are situated south of 64°N, and all the Palaeogene occurrences are situated north of 64°N. A number of periods can be discerned and related to tectonic events in the region as discussed below and illustrated in Figure 8. All correlations between the radiometric ages and the geological epochs and stages are made with reference to the geological time scale of Gradstein *et al*. (2004).

*Start of extension, 223–150 Ma (Late Triassic–Late Jurassic).* The oldest rock dated is a small aillikite dyke near Færingehavn with an age of 222.7 ± 0.3 Ma by Rb–Sr and 217.9 ± 2.9 Ma by U–Pb. The earliest recorded Mesozoic igneous activity is thus Carnian (Late Triassic). A similar aillikite dyke occurring only 6 km from the other is Jurassic (158.9 ± 0.2 Ma by Rb–Sr, 153.4 ± 8.4 Ma by U–Pb) (Tables 3 and 4). As the ages for each sample were obtained by two independent isotope systems in two different minerals, they are interpreted to be accurate and demonstrate a significant range of dyke emplacement ages within a small region. Except for the Triassic dyke and the 186 Ma Uummannaq dyke, the ages are in the narrower interval 166–150 Ma (Table 1).

The rocks from this period are aillikites, alnöites and carbonatites, all of which represent ultramafic alkaline magmas generated in very small volumes at great depths, probably at the asthenosphere–lithosphere boundary or in the deep part of the lithosphere. All arose from melting of a metasomatized mantle. The triggering of the melting could be incipient lithospheric stretching leading to localized pressure release and slight asthenospheric upwelling (Fig. 8a). Japsen *et al*. (2009) identified two events of uplift in West Greenland, one starting at 230–220 Ma and one starting at 160–150 Ma (durations cannot be distinguished). These two periods are also periods of magmatism, suggesting that pressure release as a result of erosion subsequent to uplift may also play a part; however, the uplift would have had a tectonic cause. The scattered distribution of the occurrences suggests local tectonic control, and the dyke directions do not give any indications of prevailing stress directions. The occurrences of Late Triassic to Late Jurassic rocks are scattered over a distance of 450 km between 61°24'N (Pyramidefjeld) and 65°24'N (Qaqqarsuk). The Jurassic dyke in Uummannaq Fjord at 71°13'N, 650 km farther north, may be related to incipient rifting

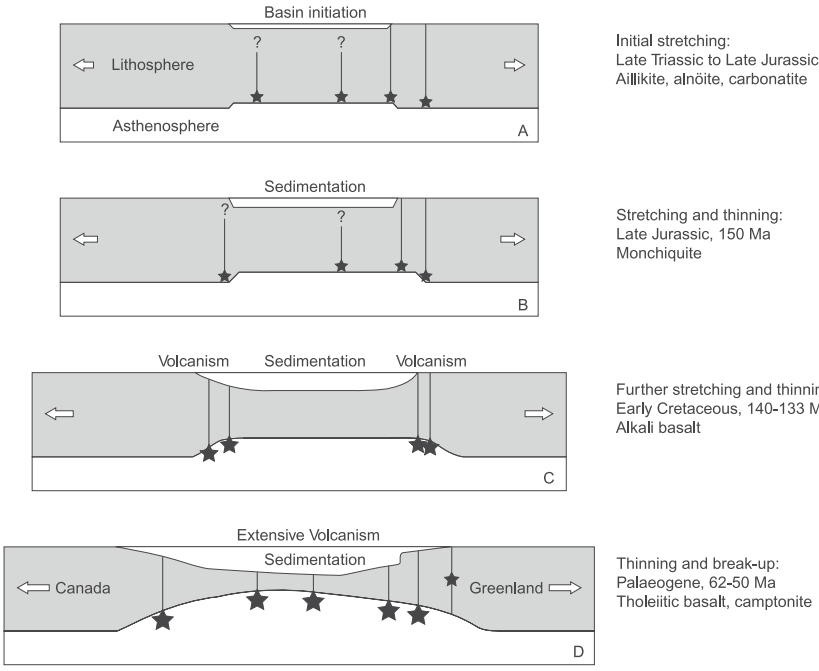


**Fig. 8.** Schematic illustrations of the progressive stages of the tectonic and magmatic development of the Labrador Sea and the Davis Strait. Stars indicate sites of melting, and the smaller and larger stars indicate smaller or larger degrees of melting.

in the Nuussuaq Basin. It is not known at present if there are any Jurassic intrusions north of 72°N where an offshore rift system in the Melville Bay extends to 76°N (Whittaker *et al*. 1997).

Igneous rocks of equivalent age on the conjugate Labrador margin are not known, but several occurrences are known from the Atlantic margin along Nova Scotia and Newfoundland (Jansa & Pe-Piper 1988; Pe-Piper *et al*. 1990, 1992; Pe-Piper & Reynolds 2000). Here, occurrences of Triassic and Jurassic alkaline and tholeiitic volcanic and intrusive igneous rocks with ages within a wide range (247–140 Ma, similar to the range in West Greenland) have been related to rifting and opening between North America and Europe, with the opening starting around 200 Ma.

Farther away, in eastern Ontario, Jurassic kimberlite magmatism around 160–140 Ma has been suggested to be related to a hotspot track (Heaman & Kjarsgaard 2000). There is no evidence of a hotspot track in the form of linear age progression in West Greenland.

*Increased extension around 150 Ma.* At around 150 Ma (Kimmeridgian), the magma composition changed to that of monchiquite, which was presumably produced by somewhat larger degrees of melting than the preceding ultramafic magmas, but still at great depths. This suggests increased extension (Fig. 8b). The melts were emplaced in a loosely defined dyke swarm around Frederikshåb Isblink that, as now known (Fig. 1), extends for 60 km with an overall NNW–SSE direction. This is the earliest evidence of a regional stress direction. These dykes are very inconspicuous in the field, and the swarm could be more extensive.

On the Labrador side, an ultramafic lamprophyric breccia diatreme at Ford's Bight near Aillik Bay has yielded microfossils of Early Jurassic to Early Cretaceous age (King & McMillan 1975). Apparently related alkaline dykes have ages around 142 Ma (Tappe *et al*. 2007).

Shales of Kimmeridgian age are important hydrocarbon source rocks in the basins on the NW European continental margin. No sediments of Jurassic age are known from the Labrador Sea (e.g. Balkwill *et al*. 1990; Chalmers *et al*. 1993; Chalmers & Pulvertaft 2001). However, seismic sections indicate the existence of 'deep' successions of unknown age, and the finding of reworked Jurassic and lower Cretaceous palynomorphs in the sediments in the Qulleq-1 well suggests that Jurassic sediments could be present at depth (Christiansen *et al*. 2001). Increased extension around 150 Ma could have provided both accommodation space in a deepening basin and sedimentary material from uplifted and eroded marginal areas.

*Regional rifting and dyking at 140–133 Ma.* Between 140 Ma and 133 Ma (Early Cretaceous, Berriasian–Valanginian to Hauterivian), the SW Greenland coast-parallel dyke swarm was emplaced in two or three stages. The more than 400 km long swarm was clearly emplaced into a coast-parallel, steeply seaward-dipping fracture system (Watt 1969), indicating a pronounced stress field and a significant regional stretching and rifting event. The basaltic alkaline to enriched tholeiitic compositions indicate much larger degrees of melting than at earlier times, and of asthenospheric mantle, probably at much shallower depths (Fig. 8c). The large dykes, up to 40 m thick (Watt 1969), must have fed a succession of lava flows that have been eroded away. The coast-parallel fracture system hosting the dykes mimics exactly the system of parallel faults on the shelf adjacent to the dyke swarm (Fig. 1), suggesting that these faults, which are thought to be slightly younger (Barremian–Aptian, Chalmers & Pulvertaft 2001), were initiated around 140 Ma. It is possible that intrusive or extrusive igneous rocks of this age also occur in the offshore areas.

On the Labrador side, and in a conjugate position relative to the SW Greenland dyke swarm, alkali basaltic volcanic rocks (the Alexis Formation) are known from seven wells covering a NW–SE stretch of about 300 km inboard of the Hopedale Basin (Umpleby 1979; Balkwill *et al*. 1990; Pe-Piper *et al*. 1990). These rocks form the oldest succession drilled on the Labrador shelf. They are biostratigraphically dated to Berriasian–Hauterivian (i.e. contemporaneous with the SW Greenland dyke swarm) and their chemical compositions are comparable with those of the SW Greenland dyke swarm. Keen *et al*. (1994) and Williamson *et al*. (1994) showed that the Alexis melts could be modelled

as formed by adiabatic decompression of the asthenosphere during stretching of the lithosphere. An asthenospheric source is also indicated for the SW Greenland swarm (Fig. 5).

*Subsidence and sedimentation at 130–120 Ma.* After the 140–133 Ma rifting event, subsidence during the Barremian and Aptian led to deposition of thick sedimentary successions in the offshore basins between Greenland and Canada: the Kitsissut sequence and the Lower Bjarni Formation respectively (e.g. Chalmers & Pulvertaft 2001). No volcanic rocks are known from this period.

*Faulting, sedimentation and magmatism around 120–100 Ma.* A major episode of faulting in the Aptian–Albian (120–100 Ma) formed a group of rotated fault-blocks, and the synrift Appat sequence and Upper Bjarni Formation were deposited (e.g. Chalmers & Pulvertaft 2001). There are traces of accompanying igneous activity at this time: the camptonite sill on Tuttutooq was emplaced at 115 Ma, and the large coast-parallel phonolite dyke at Frederikshåb Isblink was emplaced at 106 Ma. Moreover, a basalt sample dredged from a seamount in the Labrador Sea at 62°50.5'N and dated at 118 Ma may represent a dyke or a flow from the offshore area or from the coastal zone (Larsen & Dalhoff 2006). All the Cretaceous igneous rocks are feldspar-bearing and were presumably generated beneath attenuated lithosphere.

*Late Cretaceous subsidence, sedimentation and faulting at 100–65 Ma.* The faulting episode was followed by thermal subsidence of the basin during the Late Cretaceous and deposition of the Kangeq sequence and the Markland Formation. From the latest Campanian around 75 Ma and into the Maastrichtian, renewed extension and faulting occurred (e.g. Chalmers & Pulvertaft 2001). No volcanic rocks in the region are known from this period.

During the same period there was volcanic activity in the northern Canadian Arctic islands, where the Strand Fiord Formation and the Hansen Point volcanic series were erupted; this activity has been related to the formation of the oceanic Canada Basin (Embry & Osadetz 1988) and its relevance for the tectonic events in the Labrador Sea and Davis Strait is doubtful.

*Palaeogene rifting and magmatism since 65 Ma.* In the Palaeocene (65.5–55.8 Ma), rifting and lithospheric thinning proceeded to continental break-up and formation of oceanic crust (Fig. 8d). The oldest undisputedly identifiable oceanic crust in the Labrador Sea was formed within palaeomagnetic chron 27r (Chalmers & Laursen 1995). The oldest Palaeocene volcanic rocks dated from the region are tholeiitic basalts dredged from the Davis Strait High with an $^{40}Ar/^{39}Ar$ age of 63.0 ± 0.7 Ma (Larsen & Dalhoff 2006). This age is within palaeomagnetic chron 27r, which ends at 62.0 Ma (Ogg & Smith 2004). The geochemistry of these basalts indicates formation beneath a strongly attenuated continental lithospheric lid (Larsen & Dalhoff 2006). The major part of the voluminous volcanic succession onshore West Greenland from Disko to Svartenhuk Halvø was generated during the period 62–60 Ma (Storey *et al*. 1998) beneath a *c*. 100 km thick lithospheric lid (Larsen & Pedersen 2000). An extensive sill complex that extends within sediments beneath the waters of Disko Bugt and is seen on the aeromagnetic anomaly map (Rasmussen 2002) apparently forms a SE extension of the Palaeocene volcanic succession. A sill exposed in the SE corner of Disko Bugt (Grønne Ejland) is similar to the volcanic succession on Disko both with regard to age (60.9 ± 0.9 Ma, Table 2) and composition (Table 5). Onshore activity can be traced farther south to 68°N in a 110 km long NNE–SSW-trending dyke (Fig. 1) which is also compositionally similar to the volcanic rocks and is likely to have the same age. This dyke appears to form a connection between the Nuussuaq and Sisimiut basins. The area with onshore tholeiitic igneous activity thus extends southwards to around the same latitude (68°N) as does the offshore volcanic area north of the Sisimiut Basin (Fig. 1). No observations exist of Palaeogene dykes between 68°N and 66°27'N. The Itilleq dyke occurring at 66°27'N (64.1 ± 2.0 Ma, Table 2) has a composition similar to the Palaeocene volcanic rocks of the Nuussuaq Basin. This dyke was discovered by chance, and such dykes may be more widespread onshore than recognized at present.

Igneous rocks younger than 60 Ma consist of several dykes and a volcanic succession in the western volcanic areas from Nuussuaq to Svartenhuk Halvø. Most of these rocks have ages of 56.8–54.0 Ma and fairly similar compositional ranges, and the relation between them is not clear. Sill and dyke intrusions in SE Nuussuaq (56.8 ± 0.8 Ma, Table 2) were mainly emplaced along the deep eastern boundary fault of the Nuussuaq Basin. A 60 km long north–south-trending dyke in the Aasiaat district (56.1 ± 0.2 Ma, Table 2) indicates continued activity in the southern extension of the volcanic areas. The north–south-trending western Disko dyke swarm was dated at 54.3 ± 0.3 Ma by Storey *et al*. (1998). Some of the young dykes may be feeders for the young volcanic succession that is now known only from the western volcanic areas but that may extend into the offshore basins. It may also originally have covered larger areas onshore.

*Palaeogene alkaline rocks*. Except for the Itilleq dyke, Palaeogene tholeiitic rocks south of 68°N are known only from offshore areas on the Nukik platform and the Maniitsoq and Hecla Highs (Larsen & Dalhoff 2006) (Fig. 1). Palaeogene onshore igneous activity in the southern areas produced alkaline rocks: the camptonite dyke swarms in the Søndre Isortoq and Godthåbsfjord areas and the single alkali basalt dyke at Søndre Isortoq. The period of formation of these rocks is long, 58–51 Ma, which is the same as the period found for the offshore volcanic area of the Hecla High (Larsen & Dalhoff 2006). The alkali basalt dyke is the oldest (58.5 ± 0.64 Ma, Table 2). The two camptonite swarms, situated 120 km apart, gave significantly different ages of 55.7 ± 0.6 Ma (Søndre Isortoq) and 51.7 ± 0.9 Ma (Godthåbsfjord). All these rocks require a metasomatized mantle source (Fig. 5). The camptonites were generated at shallow levels (Figs 6 and 7), apparently well within the lithosphere. It is conceivable that metasomatic conditioning of the lithosphere, possibly starting in the asthenosphere, took place early in the Palaeocene. The metasomatized regions then constituted reservoirs in which melting could subsequently be triggered easily during events of lithospheric stretching. During such events, extension in the thinned offshore areas could be sufficiently high to produce tholeiitic basalts, whereas simultaneous extension beneath the thicker continent was much less but enough to trigger melting of the metasomatized regions. The onshore and offshore igneous areas are situated at similar latitudes (Fig. 1) but no direct tectonic link between them is apparent.

In the northern area between Disko and Svartenhuk Halvø, alkaline rocks were also formed at late stages. The 34.5 Ma monchiquites and camptonites on Ubekendt Ejland and also the alkaline 28 Ma volcanic plug just west of Disko could have formed by melting of previously metasomatized lithosphere as envisaged for the camptonites in the southern areas. Their presence indicates that tectonic events that triggered melting took

place during an extended period after the main igneous event, lasting until the Oligocene.

## Conclusions

Occurrences of Mesozoic to Palaeogene igneous rocks in West Greenland can be related to events during the period when the continent underwent stretching, rifting, and break-up, with concomitant development of offshore basins. These rocks therefore provide evidence on the history of formation of the offshore basins, and the record extends from 223 Ma (Late Triassic) to 28 Ma (Oligocene).

The period 223–150 Ma (Late Triassic to Late Jurassic) is characterized by production of scattered small volumes of highly alkaline, volatile-rich melts: aillikites, alnöites and carbonatites, formed at very low degrees of melting in deep, metasomatized parts of the thick lithosphere.

In the Late Jurassic around 150 Ma (Kimmeridgian), the degree of melting increased and monchiquitic melts were produced, suggesting increased extension. These rocks form an at least 60 km long NNW–SSE-oriented dyke swarm around Frederikshåb Isblink, giving the earliest indication of a directional stress field.

In the Early Cretaceous, 140–133 Ma (Valanginian–Hauterivian), the melts were alkaline to enriched tholeiitic basalts produced at still larger degrees of melting, suggesting considerable lithospheric attenuation. They were emplaced in a 400 km long coast-parallel fracture system, and the regional extensional stress field was intense. The alkali basalts of the Alexis Formation on the conjugate Canadian margin were presumably formed at this time.

During the rest of the Cretaceous, onshore igneous activity was sparse but two occurrences dated at 115 Ma and 105 Ma are known. Cretaceous igneous rocks may also be present in the offshore areas.

In the Palaeogene, continental break-up and extrusion of voluminous tholeiitic flood basalts took place in the period 62–60 Ma. Sills in Disko Bugt form an intrusive southeastern extension of the volcanic areas, and a large dyke in the Aasiaat region appears to form a link between the Nuussuaq and Sisimiut Basins. Dykes with ages of 57–51 Ma indicate that younger volcanic activity was more widespread than present outcrops suggest.

Two small alkaline dyke swarms dated at 58–51 Ma were formed by shallow melting in the lithosphere. They may have resulted from local stresses set up repeatedly by minor lithospheric adjustments.

This work was partly supported by the Bureau of Minerals and Petroleum, Nuuk. Numerous geologists have over the years contributed with samples and information about the dykes. Contributions from and discussions with U. Árting, S. Bernstein, A. Garde, K. Hansen, A. Higgins, M. Lind, H. K. Olsen, A. K. Pedersen, T. M. Rasmussen, C. Pulvertaft, K. Secher, A. Steenfelt, B. Upton, and S. Watt are gratefully acknowledged. J. Huard patiently recalculated all the $^{40}Ar/^{39}Ar$ ages to the new (2008) age for the FCT monitor and compiled the data table. Publication was authorized by the Geological Survey of Denmark and Greenland.

## References

Andrews, J.R. & Emeleus, C.H. 1971. Preliminary account of kimberlite intrusions from the Frederikshåb district, South-West Greenland. *Rapport Grønlands Geologiske Undersøgelse*, **31**, 1–26.

Árting, U.E. 2004. *A petrological study of basic dykes and sills of assumed Palaeoproterozoic age in central West Greenland*. MSc thesis, University of Copenhagen.

Balkwill, H.R., McMillan, N.J., Maclean, B., Williams, G.L. & Srivastava, S.P. 1990. Geology of the Labrador Shelf, Baffin Bay, and Davis Strait. *In:* Keen, M.J. & Williams, G.L. (eds) *Geology of the Continental Margin of Eastern Canada*. Geological Survey of Canada, Geology of Canada, **2**, 293–348.

Best, M.G. 2006. *Igneous and Metamorphic Petrology*, 2nd edn. Blackwell, Oxford.

Bridgwater, D. 1970. A compilation of K/Ar age determinations on rocks from Greenland carried out in 1969. *Rapport Grønlands Geologiske Undersøgelse*, **28**, 47–55.

Chalmers, J.A. 1991. New evidence on the structure of the Labrador Sea/Greenland continental margin. *Journal of the Geological Society, London*, **148**, 899–908.

Chalmers, J.A. & Laursen, K.H. 1995. Labrador Sea: The extent of continental crust and the timing of the start of sea-floor spreading. *Marine and Petroleum Geology*, **12**, 205–217.

Chalmers, J.A. & Pulvertaft, T.C.R. 2001. Development of the continental margins of the Labrador Sea: a review. *In:* Wilson, R.C.L., Whitmarsh, R.B., Taylor, B. & Froitzheim, N. (eds) *Non-volcanic Rifting of Continental Margins: a Comparison of Evidence from Land and Sea*. Geological Society, London, Special Publications, **187**, 77–105.

Chalmers, J.A., Pulvertaft, T.C.R., Christiansen, F.G., Larsen, H.C., Laursen, K.H. & Ottesen, T.G. 1993. The southern West Greenland continental margin: rifting history, basin development, and petroleum potential. *In:* Parker, J.R. (ed.) *Petroleum Geology of Northwest Europe: Proceedings of the 4th Conference*. Geological Society, London, 915–931.

Christiansen, F.G., Bojesen-Koefoed, J., Chalmers, J.A., *et al.* 2001. Petroleum geological activitites in West Greenland in 2000. *Geology of Greenland Survey Bulletin*, **189**, 24–33.

Clarke, D.B., Muecke, G.K. & Pe-Piper, G. 1983. The lamprophyres of Ubekendt Ejland, West Greenland: products of renewed partial melting or extreme differentiation? *Contributions to Mineralogy and Petrology*, **83**, 117–127.

Creaser, R.A., Grütter, H., Carlson, J. & Crawford, B. 2004. Macrocrystal phlogopite Rb–Sr dates for the Ekati property kimberlites, Slave Province, Canada: evidence for multiple intrusive episodes in the Paleocene and Eocene. *Lithos*, **76**, 399–414.

Duggen, S., Hoernle, K., van den Bogaard, P. & Garbe-Schönberg, D. 2005. Post-collisional transition from subduction- to intraplate-type magmatism in the westernmost Mediterranean: evidence for continental-edge delamination of subcontinental lithosphere. *Journal of Petrology*, **46**, 1155–1201.

Embry, A.F. & Osadetz, K.G. 1988. Stratigraphy and tectonic significance of Cretaceous volcanism in the Queen Elizabeth Islands, Canadian Arctic Archipelago. *Canadian Journal of Earth Sciences*, **25**, 1209–1219.

Frei, D., Hutchison, M.T., Gerdes, A. & Heaman, L.M. 2008. Common-lead corrected U–Pb age dating of perovskite by laser ablation–magnetic sectorfield ICP-MS. *In: Ninth International Kimberlite Conference, Extended Abstracts*, No. 9IKC-A-00216.

Funck, T., Jackson, H.R., Louden, K.E. & Klingelhöfer, F. 2007. Seismic study of the transform-rifted margin in Davis Strait between Baffin Island (Canada) and Greenland: What happens when a plume meets a transform. *Journal of Geophysical Research*, **112**, B04402, doi:10.1029/2006JB004308.

Garrit, D., Griffin, W.L., Larsen, L.M. & O'Reilly, S. 1997. Ultramafic xenoliths and mantle-derived megacrysts from the Archaean and Proterozoic lithospheric mantle in West Greenland. (EUG 9, Strasbourg.) *Terra Nova*, **9**, 75.

Gradstein, F.M., Ogg, J.G. & Smith, A.G. (eds) 2004. *A Geologic Time Scale 2004*. Cambridge University Press, Cambridge.

Green, D.H. & Ringwood, A.E. 1967. The genesis of basaltic magmas. *Contributions to Mineralogy and Petrology*, **15**, 103–190.

Hansen, H. 2002. *Description of rock samples from a West Greenland drill core*. Danmarks og Grønlands Geologiske Undersøgelse Rapport, **2002/109**.

Hansen, K. 1979. *Lamprofyrgange fra Frederikshåbs Isblink, syd vest Grønland*. MSc thesis, University of Copenhagen.

Hansen, K. 1980. Lamprophyres and carbonatitic lamprophyres related to rifting in the Labrador Sea. *Lithos*, **13**, 145–152.

Hansen, K. & Larsen, O. 1974. K/Ar age determinations on Mesozoic lamprophyre dykes near Ravns Storø, Fiskenæsset Region, southern West Greenland. *Rapport Grønlands Geologiske Undersøgelse*, **66**, 9–11.

Heaman, L.M. & Kjarsgaard, B.A. 2000. Timing of eastern North American kimberlite magmatism: continental extension of the Great Meteor hotspot track? *Earth and Planetary Science Letters*, **178**, 253–268.

Henderson, G., Schiener, E.J., Risum, J.B., Croxton, C.A. & Andersen, B.B. 1981. The west Greenland Basin. *In:* Kerr, J.W. (ed.) *Geology of the North Atlantic Borderlands*. Memoir, Canadian Society of Petroleum Geologists, **7**, 399–428.

Jansa, L.F. & Pe-Piper, G. 1988. Middle Jurassic to Early Cretaceous igneous rocks along eastern North American continental margin. *AAPG Bulletin*, **72**, 347–366.

Japsen, P., Bonow, J.M., Green, P.F., Chalmers, J.A. & Lidmar-Bergström, K. 2009. Formation, uplift and dissection of planation surfaces at passive continental margins—a new approach. *Earth Surface Processes and Landforms*, doi:10.1002/esp.1766.

Keen, C.E., Loncarevic, B.D., Reid, I., Woodside, J., Haworth, R.T. & Williams, H. 1990. Tectonic and geophysical overview. *In:* Keen, M.J. & Williams, G.L. (eds) *Geology of the Continental Margin of Eastern Canada*. Geological Survey of Canada, Geology of Canada, **2**, 31–85.

Keen, C.E., Courtney, R.C., Dehler, S.A. & Williamson, M.-C. 1994. Decompression melting at rifted margins: comparison of model predictions with the distribution of igneous rocks on the eastern Canadian margin. *Earth and Planetary Science Letters*, **121**, 403–416.

King, A.F. & McMillan, N.J. 1975. A Mid-Mesozoic breccia from the coast of Labrador. *Canadian Journal of Earth Science*, **12**, 44–51.

Koppers, A.A.P. 2002. ArArCALC; software for $^{40}Ar/^{39}Ar$ age calculations. *Computers and Geosciences*, **28**, 605–619.

Kuiper, K.F., Deino, A., Hilgen, F.J., Krijgsman, W., Renne, P.R. & Wijbrans, J.R. 2008. Synchronizing rock clocks of Earth history. *Science*, **320**, 500–504.

Kushiro, I. 1968. Compositions of magmas formed by partial zone melting of the Earth's upper mantle. *Journal of Geophysical Research*, **73**, 619–634.

Kystol, J. & Larsen, L.M. 1999. Analytical procedures in the Rock Geochemical Laboratory of the Geological Survey of Denmark and Greenland. *Geology of Greenland Survey Bulletin*, **184**, 59–62.

Larsen, L.M. 2006. *Mesozoic to Palaeogene dyke swarms in West Greenland and their significance for the formation of the Labrador Sea and the Davis Strait*. Danmarks og Grønlands Geologiske Undersøgelse Rapport, **2006/34**.

Larsen, L.M. & Dalhoff, F. 2006. *Composition, age, and geological and geotectonic significance of igneous rocks dredged from the northern Labrador Sea and the Davis Strait*. Danmarks og Grønlands Geologiske Undersøgelse Rapport, **2006/43**.

Larsen, L.M. & Pedersen, A.K. 2000. Processes in high-Mg high-*T* magmas: Evidence from olivine, chromite and glass in Paleogene picrites from West Greenland. *Journal of Petrology*, **41**, 1071–1098.

Larsen, L.M. & Rex, D.C. 1992. A review of the 2500 Ma span of alkaline–ultramafic, potassic and carbonatitic magmatism in West Greenland. *Lithos*, **28**, 367–402.

Larsen, L.M., Rex, D.C. & Secher, K. 1983. The age of carbonatites, kimberlites and lamprophyres from southern West Greenland: recurrent alkaline magmatism during 2500 million years. *Lithos*, **16**, 215–221.

Larsen, L.M., Rex, D.C., Watt, W.S. & Guise, P.G. 1999. $^{40}Ar–^{39}Ar$ dating of alkali basaltic dykes along the south-west coast of Greenland: Cretaceous and Tertiary igneous activity along the eastern margin of the Labrador Sea. *Geology of Greenland Survey Bulletin*, **184**, 19–29.

Larsen, O. & Møller, J. 1968. K/Ar age determinations from western Greenland I. Reconnaissance programme. *Rapport Grønlands Geologiske Undersøgelse*, **15**, 82–86.

Le Maitre, R.W. (ed.) 2002. *Igneous Rocks, A Classification and Glossary of Terms, Recommendations of the IUGS Subcommission on the Systematics of Igneous Rocks*, 2nd edn. Cambridge University Press, Cambridge.

Ludwig, K.R. 2003. Mathematical–statistical treatment of data and errors for $^{230}Th/U$ geochronology. *In:* Bourdon, B., Henderson, G.M., Lundstrom, C.C. & Turner, S.P. (eds) *Uranium-series Geochemistry.* Reviews in Mineralogy and Geochemistry, **52**, 631–656.

McDonough, W.F. & Sun, S.-S. 1995. The composition of the Earth. *Chemical Geology*, **120**, 223–253.

Menzies, M.A. 1990. Archaean, Proterozoic, and Phanerozoic lithosphere. *In:* Menzies, M.A. (ed.) *Continental Mantle*. Oxford Monograph on Geology and Geophysics, **16**, 67–86.

Ogg, J.G. & Smith, A.G. 2004. The geomagnetic polarity time scale. *In:* Gradstein, F.M., Ogg, J.G. & Smith, A.G. (eds) *A Geological Time Scale 2004*. Cambridge University Press, Cambridge, 63–86.

Ottley, C.J., Pearson, D.G. & Irvine, G.J. 2003. A routine method for the dissolution of geological samples for the analysis of REE and trace elements via ICP-MS. *In:* Holland, J.G. & Tanner, S.D. (eds) *Plasma Source Mass Spectrometry: Applications and Emerging Technologies*. Royal Society of Chemistry, Cambridge, 221–230.

Pe-Piper, G. & Reynolds, P.H. 2000. Early Mesozoic alkaline mafic dykes, southwestern Nova Scotia, Canada, and their bearing on Triassic–Jurassic magmatism. *Canadian Mineralogist*, **38**, 217–232.

Pe-Piper, G., Piper, D.J.W., Keen, M.J. & McMillan, N.J. 1990. Igneous rocks of the continental margin. *In:* Keen, M.J. & Williams, G.L. (eds) *Geology of the Continental Margin of Eastern Canada*. Geological Survey of Canada, Geology of Canada, **2**, 75–85.

Pe-Piper, G., Jansa, L.F. & Lambert, R.St.J. 1992. Early Mesozoic magmatism on the eastern Canadian margin: Petrogenetic and tectonic significance. *In:* Puffer, J.H. & Ragland, P.C. (eds) *Eastern North American Mesozoic Magmatism*. Geological Society of America, Special Papers, **268**, 13–36.

Rasmussen, T.M. 2002. Aeromagnetic survey in central West Greenland: Project Aeromag 2001. *Geology of Greenland Survey Bulletin*, **191**, 67–72.

Roest, W.R. & Srivastava, S.P. 1989. Sea-floor spreading in the Labrador Sea: A new reconstruction. *Geology*, **17**, 1000–1003.

Salters, V.J.M. & Stracke, A. 2004. Composition of the depleted mantle. *Geochemistry, Geophysics, Geosystems*, **5**, doi:10.1029/2003GC000597.

Sand, K.K., Waight, T.E., Pearson, D.G., Nielsen, T.F.D., Makovicky, E. & Hutchison, M.T. 2009. The lithospheric mantle below southern West Greenland: a geothermobarometric approach to diamond potential and mantle stratigraphy. *Lithos*, doi:10.1016/j.lithos.2009.05.012.

Secher, K., Heaman, L.M., Nielsen, T.F.D., Jensen, S.M., Schjøth, F. & Creaser, R.A. 2009. Timing of kimberlite, carbonatite, and ultramafic lamprophyre emplacement in the alkaline province located 64°–67°N in southern West Greenland. *Lithos*, doi:10.1016/j.lithos.2009.04.035.

Srivastava, S.P. 1978. Evolution of the Labrador Sea and its bearing on the early evolution of the North Atlantic. *Geophysical Journal of the Royal Astronomical Society*, **52**, 313–357.

Stacey, J.S. & Kramers, J.D. 1975. Approximation of terrestrial lead isotope evolution by a two-stage model. *Earth and Planetary Science Letters*, **26**, 207–221.

Steenfelt, A., Hollis, J.A. & Secher, K. 2006. The Tikiusaaq carbonatite: a new Mesozoic intrusive complex in southern West Greenland. *Geological Survey of Denmark and Greenland Bulletin*, **10**, 41–44.

Steiger, R. H. & Jäger, E. 1977. Subcommission on geochronology: convention on the use of decay constants in geo- and cosmochronology. *Earth and Planetary Science Letters*, **36**, 359–362.

Storey, M., Duncan, R.A., Pedersen, A.K., Larsen, L.M. & Larsen, H.C. 1998. $^{40}Ar/^{39}Ar$ geochronology of the West Greenland Tertiary volcanic province. *Earth and Planetary Science Letters*, **160**, 569–586.

Tappe, S., Foley, S.F., Jenner, G.J. & Kjarsgaard, B.A. 2005. Integrating ultramafic lamprophyres into the IUGS classification of igneous rocks: rationale and implications. *Journal of Petrology*, **46**, 1893–1900.

Tappe, S., Foley, S.F., Stracke, A., Romer, R.L., Kjarsgaard, B.A., Heaman, L.M. & Joyce, N. 2007. Craton reactivation on the Labrador Sea margins: $^{40}Ar/^{39}Ar$ age and Sr–Nd–Hf–Pb isotope constraints from alkaline and carbonatite intrusives. *Earth and Planetary Science Letters*, **256**, 433–454.

Tappe, S., Steenfelt, A., Heaman, L.M., Simonetti, A. & Creaser, R.A. 2009. The newly discovered Tikiusaaq carbonatite–aillikite occurrence, West Greenland, and some remarks on carbonatite–kimberlite relationships. *Lithos*, doi:10.1016/j.lithos.2009.03.002.

Turner, S.P., Platt, J.P., George, R.M.M., Kelly, S.P., Pearson, D.G. & Nowell, G.M. 1999. Magmatism associated with orogenic collapse of the Betic–Alboran domain, SE Spain. *Journal of Petrology*, **40**, 1011–1036.

Umpleby, D.C. 1979. *Geology of the Labrador Shelf*. Geological Survey of Canada Paper, **79-13**.

Walter, M.J. 1998. Melting of garnet peridotite and the origin of komatiite and depleted lithosphere. *Journal of Petrology*, **39**, 29–60.

Watt, W.S. 1969. The coast-parallel dike swarm of southwest Greenland in relation to the opening of the Labrador Sea. *Canadian Journal of Earth Sciences*, **6**, 1320–1321.

Whittaker, R.C., Hamann, N.E. & Pulvertaft, T.C.R. 1997. A new frontier province offshore northwest Greenland: structure, basin development, and petroleum potential of the Melville Bay area. *AAPG Bulletin*, **81**, 978–998.

Williamson, M.-C., Courtney, R.C., Keen, C.E. & Dehler, S.A. 1994. Relationship between crustal deformation and magmatism in rift zones: modelling approach and applications to the eastern Canadian margin. *Geological Survey of Canada, Current Research*, **1994-E**, 251–258.

Wilson, M. 1989. *Igneous Petrogenesis. A Global Tectonic Approach*. Unwin Hyman, London.

Received 17 March 2009; revised typescript accepted 6 July 2009.
Scientific editing by Rob Strachan.